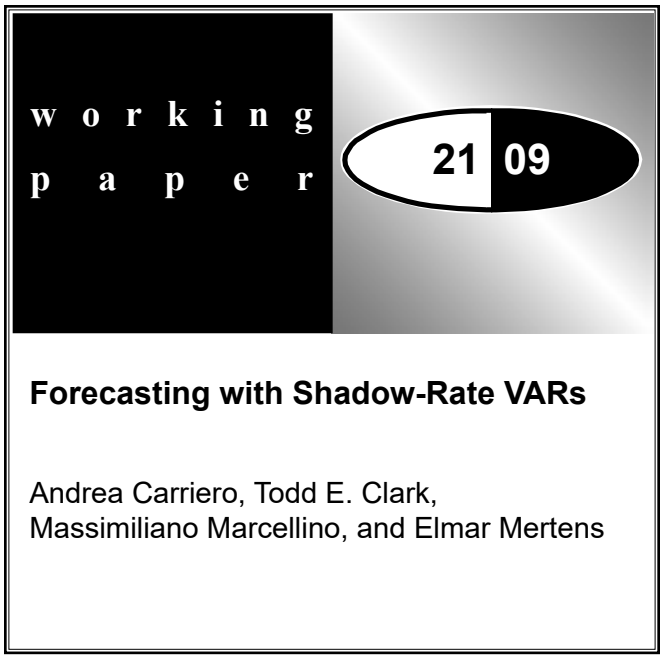

Forecasting with Shadow-Rate VARs

Andrea Carriero, Todd E. Clark,
Massimiliano Marcellino, and Elmar Mertens

FEDERAL RESERVE BANK OF CLEVELAND

ISSN: 2573-7953

Working Paper 21-09 March 2021

Forecasting with Shadow-Rate VARs

Andrea Carriero, Todd E. Clark, Massimiliano Marcellino, and Elmar Mertens

Interest rate data are an important element of macroeconomic forecasting. Projections of future interest rates are not only an important product themselves, but also typically matter for forecasting other macroeconomic and financial variables. A popular class of forecasting models is linear vector autoregressions (VARs) that include shorter- and longer-term interest rates. However, in a number of economies, at least shorter-term interest rates have now been stuck for years at or near their effective lower bound (ELB), with longer-term rates drifting toward the constraint as well. In such an environment, linear forecasting models that ignore the ELB constraint on nominal interest rates appear inept. To handle the ELB on interest rates, we model observed rates as censored observations of a latent shadow-rate process in an otherwise standard VAR setup. The shadow rates are assumed to be equal to observed rates when above the ELB. Point and density forecasts for interest rates (short term and long term) constructed from a shadow-rate VAR for the US since 2009 are superior to predictions from a standard VAR that ignores the ELB. For other indicators of financial conditions and measures of economic activity and inflation, the accuracy of forecasts from our shadow-rate specification is on par with a standard VAR that ignores the ELB.

Keywords: Macroeconomic forecasting, effective lower bound, term structure, censored observations.

JEL classification codes: C34, C53, E17, E37, E43, E47.

Suggested citation: Carriero, Andrea, Todd E. Clark, Massimiliano Marcellino, and Elmar Mertens. 2021. "Forecasting with Shadow-Rate VARs." Federal Reserve Bank of Cleveland, Working Paper No. 21-09. https://doi.org/10.26509/frbc-wp-202109.

Andrea Carriero is at Queen Mary University of London (a.carriero@qmul.ac.uk). Todd E. Clark is at the Federal Reserve Bank of Cleveland (todd.clark@clev.frb.org). Massimiliano Marcellino is at Bocconi University, IGIER, and CEPR (massimiliano.marcellino@unibocconi.it). Elmar Mertens is at Deutsche Bundesbank (elmar.mertens@bundesbank.de). The authors gratefully acknowledge helpful suggestions and comments received from Refet Gürkaynak, Emanuel Mönch, Frank Schorfheide, Harald Uhlig, and seminar participants at the Bank of England, Bocconi University, Deutsche Bundesbank, and Penn. Additional results are provided in an online appendix.

1 Introduction

Interest rate data are an important element of macroeconomic forecasting. Projections of future interest rates are not only an important product themselves, but also typically matter for forecasting other macroeconomic and financial variables. A popular class of forecasting models is linear vector autoregressions (VARs) that include shorter- and longer-term interest rates. However, in a number of economies, at least shorter-term interest rates have now been stuck for years at or near their effective lower bound (ELB), with longer-term rates drifting toward the constraint as well. In such an environment, linear forecasting models that ignore the ELB constraint on nominal interest rates can be problematic along various dimensions.

For concreteness, we consider the case of the US, where the Federal Open Market Committee (FOMC) has set the target range for the federal funds rate no lower than 0-25 basis points. The Committee maintained this target range over the seven-year stretch from December 2008 through December 2015, after the Great Recession, and has again maintained this target range since March 2020, when the COVID-19 pandemic initiated a recession, and indicated an intention to maintain the range for an extended period. Considering other economies, the ELB may even be a bit below zero, with several central banks pursuiing so-called negative interest rate policies (NIRP), albeit still at levels close to zero.[1] Similar to the US experience, policy rates observed under NIRP so far appear constrained to fall much below zero.

In such an environment, a fundamental challenge for forecasting models is to appropriately capture the existence of an ELB on interest rates and the resulting asymmetries in predictive densities not only for interest rates, but also likely other economic variables. The likelihood of a binding ELB may also affect economic dynamics and co-movements between

[1]For example, the Swiss National Bank is targeting a level of -75 basis points for its policy rate, while the European Central Bank has maintained a deposit rate of -50 basis points since September 2019, the culmination of a series of steps starting in December 2011 to gradually lower the rate from 25 basis points. The repo rate of the Swedish Riksbank has been at or below 25 basis points since October 2014, bottoming out at -50 basis points from February 2016 to January 2019, and remaining at 0 through 2020. One of the most extensive episodes of monetary policy near the ELB has occurred in Japan, where policy rates have been near zero since 2008, with the current policy rate at -10 basis points since 2016.

different variables more broadly. At a mechanical level, the existence of an ELB calls for treating nominal interest rates as variables whose observations are censored at their lower bound.[2] So far the literature has discussed a number of potential remedies to ELB complications, in some cases taking a short-cut that avoids dealing with censoring. From a macroeconomic perspective, Swanson and Williams (2014) have argued that it may be sufficient to track longer-term nominal interest rates, as long as their dynamics have remained unaffected by a binding ELB on shorter-term rates, and this has been done by, for example, Debortoli, Gali, and Gambetti (2019). However, by 2020, even 10-year US Treasury yields had fallen below 1 percent, with 5-year yields hovering just above 25 basis points.

In contrast, the finance literature has derived important implications of the ELB for the entire term structure of interest rates. Following the seminal work of Black (1995), the term structure literature views the ELB as a censoring constraint on nominal interest rates (as we do), from which no-arbitrage restrictions are derived for yields of all maturities (which we do not). The resulting restrictions are, however, non-trivial and have mostly been implemented for models with state dynamics that are affine, homoskedastic, and time-invariant; see, for example, Christensen and Rudebusch (2015), Krippner (2015), Bauer and Rudebusch (2016), and Wu and Xia (2016).[3]

An upshot of the term structure literature is the availability of shadow-rate estimates, such as those regularly updated by Wu and Xia (2016). Indeed, one possible choice for applied work is to plug in these shadow-rate estimates as data points for the nominal short-term interest rate during an ELB episode. However, while convenient, this plug-in approach risks a generated regressor problem that could be substantial, as argued by, for example, Krippner (2020). Mavroeidis (2020) notes that a plug-in approach rules out consistent estimation and valid inference with a VAR, due to estimation error in the shadow rate that is often highly

[2]Alternatively, a bounded process for the nominal interest rate could be specified as in Bäurle, et al. (2016), Chan and Strachan (2014), Iwata and Wu (2006), and Nakajima (2011) without a role for an uncensored state variable to drive the nominal interest rate.

[3]Kim and Singleton (2012) also consider a quadratic-Gaussian specification with a shadow rate and find that it fits data for Japan from 1995 to 2008 as well as a shadow-rate specification in the tradition of Black (1995).

autocorrelated and not asymptotically negligible. Shadow-rate estimates are model-specific objects, fitted to best capture the dynamics of observed data through the lens of the model, and can be quite sensitive to model choices (Christensen and Rudebusch (2015); Krippner (2020)). An obvious remedy to these considerations is to integrate the shadow-rate inference into the forecasting model.

In this paper, we develop a shadow-rate approach for accommodating the ELB in macroeconomic VARs commonly used in forecasting. To do so, we extend the unobserved components model of Johannsen and Mertens (2021) to the general VAR setting. To handle the ELB on interest rates, we model observed rates as censored observations of a latent shadow-rate process in an otherwise standard VAR setup. The shadow rates are assumed to be equal to observed rates when above the ELB. Our approach is made feasible by the development of a shadow rate algorithm more computationally efficient than that of Johannsen and Mertens (2021). In particular, we use a sequential procedure, which is embedded in a Markov chain Monte Carlo (MCMC) sampler, to generate posterior draws from the latent shadow rate process that is computationally much more efficient than the rejection sampling used by Johannsen and Mertens (2021). We apply our shadow-rate approach to a medium-scale Bayesian VAR (BVAR) with stochastic volatility that has already been shown to generate competitive forecasts when ignoring the ELB (e.g., Carriero, Clark, and Marcellino (2019)).[4]

In our results, forecasts for interest rates obtained from a shadow-rate VAR for the US since 2009 are clearly superior, in terms of both point and density forecasts, to predictions from a standard VAR that ignores the ELB. These interest rates include not only the federal funds rate but also longer-term bond yields. For other indicators of financial conditions and measures of economic activity and inflation, the accuracy of forecasts from our shadow-rate specification is on par with a standard VAR that ignores the ELB. Overall, our shadow-rate

[4]Apart from modeling interest rates at the ELB treatment, our setup follows Carriero, Clark, and Marcellino (2019), who describe efficient MCMC methods for the estimation of a VAR with stochastic shock volatilities when applied to a larger variable vector as in our application. Other studies documenting the relevance of heteroskedasticity in VARs are Clark (2011), D'Agostino, Gambetti, and Giannone (2013), Clark and Ravazzolo (2015), and Chan and Eisenstat (2018).

specification successfully addresses the ELB and improves interest rate forecasts without harming a standard VAR's ability to forecast a range of other variables. In this respect, our proposed approach could be seen as a helpful tool for preserving the practical value of VARs for forecasting. In practical settings, presented with forecasts from standard VARs in which interest rates fall below the ELB, consumers of forecasts could question the reliability or plausibility of the forecasts of the other variables of interest. To these consumers, forecasts of macroeconomic variables from a shadow-rate VAR that obeys the ELB could be seen as more reliable or plausible even if their historical accuracy was no greater than that achieved by a standard VAR ignoring the ELB.

As a simpler alternative to our shadow-rate VAR, a researcher might be interested in estimating a standard VAR and merely truncating its predictive densities for nominal interest rates to capture the ELB.[5] Indeed, in terms of average forecast accuracy for the 2009-2020 period, we find important benefits for federal funds forecasts from such an approach. But, when the policy rate is at the ELB, such an approach tends to place non-negligible odds on an imminent departure from the bound at every period, which has not been borne out by the relatively long-lived ELB episode seen in the US after 2008 (and other countries outside our sample, as well). Moreover, in average forecast accuracy, this approach does not improve the accuracy of forecasts of other interest rates. In addition, we compare forecasts from our shadow-rate VAR against those obtained from the aforementioned plug-in approach, where external shadow-rate estimates, like those from Wu and Xia (2016) or Krippner (2013, 2015), are used as data, in place of the actual short-term interest rate, in an otherwise standard VAR. As reported below, we find consistent benefits for point and density forecasting from using the shadow-rate VAR across a wide range of variables.

To relate our approach to other shadow-rate work, we share with the term structure literature on shadow-rate models the approach of modeling nominal interest rates as censored

[5]In this truncated VAR, forecasts for other variables are also affected by the truncation of predictive densities for nominal interest rates through their effects in dynamic simulations of future values of all variables included in the VAR system.

variables, but we do not enforce any specific no-arbitrage (or other structural) restrictions. As such, our approach is part of the literature that uses VARs (or other reduced-form models) to derive forecasts and expectational errors of financial and economic variables without imposing the restrictions of a specific structural model (such as an affine term structure or DSGE model). Should the data satisfy such restrictions, they will also be embodied in estimates derived from a more generic reduced-form model. The potential loss in the efficiency of forecasts that do not expressively enforce such restrictions can be offset by a gain in robustness obtained from not imposing restrictions that are false. In fact, as argued by Joslin, Le, and Singleton (2013), the possible gains for forecasting from imposing restrictions from the true term structure model may be small. Moreover, as in Johannsen and Mertens (2021), economic forecasters may be interested in using time series models that allow for features, such as time-varying parameters and stochastic volatilities, that may be harder to embed in a formal no-arbitrage model.

In the context of structural VAR models (SVARs), Mavroeidis (2020) and Aruoba, et al. (2021) consider shadow-rate approaches to identify and estimate impulse responses to monetary policy shocks. Mavroeidis (2020) discusses various specification choices for the underlying reduced-form VAR model, similar to some that we also evaluate. In contrast, Aruoba, et al. (2021) limit attention to settings where VAR forecasts depend on lagged actual rates, but not lagged shadow rates.[6] We differ from these studies in focusing on the implementation of the shadow-rate approach in a reduced-form Bayesian VAR (with stochastic volatility), and we evaluate its application to a medium-scale forecasting problem.[7] To focus on this

[6]In Aruoba, et al. (2021), the shadow rate arises only contemporaneously when the VAR vector is shocked. Similarly, Iwata and Wu (2006), Berg (2017), and Chan and Strachan (2014) consider only censoring of the VAR's left-hand side variables, without tracking the underlying, uncensored shadow rate as a potential predictor. The inclusion of lagged shadow rates as VAR predictors could, however, be potentially relevant as a means of tracking make-up policies at the ELB, as discussed by, among others, Reifschneider and Williams (2000), Gust, et al. (2017), and Billi (2020).

[7]Johannsen and Mertens (2021) provide an out-of-sample forecast evaluation for short- and long-term nominal interest rates in a model smaller than our VARs, and find their unobserved components shadow-rate model to be competitive with the no-arbitrage model of Wu and Xia (2016), but do not consider forecasts of other variables. Gonzalez-Astudillo and Laforte (2020) embed a shadow-rate model in an unobserved components model and report improved point forecasts for economic and financial variables from the shadow-rate approach.

question, we abstract from uncertainty and possible drift in the level of the ELB, which appears to be a reasonable approach at least in the context of the US.[8]

The remainder of this paper is structured as follows: Section 2 describes the modeling and estimation of our shadow-rate VARs. Section 3 details the data used in our empirical application. Section 4 presents shadow-rate estimates and resulting interest rate projections. Section 5 provides a forecast evaluation, and Section 6 concludes.

2 Shadow-rate VARs

This section contrasts our shadow-rate approach with a conventional VAR, as well as related alternatives. Throughout, we take the value of the lower bound, denoted ELB, as a given and known constant. For brevity, we use the singular to refer to "the" nominal interest rate, i_t, and its associated shadow rate, s_t. The framework is easily extended to the cases where the ELB is binding for N_s interest rates of multiple maturities, which might arise, for example, in the case of aggressive forward guidance or yield curve control.

A central element of our approach is to relate actual and shadow rates via a censoring equation known from Black (1995):

$$i_t = \max\left(ELB, s_t\right). \tag{1}$$

As in the no-arbitrage literature on the term structure of interest rates (surveyed in Section 1), the censoring function (1) implies that the shadow rate is observed and equal to the actual interest rate when the latter is above the ELB.[9] When the ELB is binding, so

[8] In our empirical application on US data, we consider the ELB to have a constant and known value of 25 basis points, consistent with other studies, such as Bauer and Rudebusch (2016), Wu and Xia (2016), and Johannsen and Mertens (2021). Considering the euro area, for example, Wu and Xia (2020) model and estimate a stochastic downward drift in the ELB level.

[9] The property that the shadow rate is identical to the actual rate when above the ELB makes our approach based on Black (1995) distinct from others, like Lombardi and Zhu (2018), that define shadow rates more broadly as a common factor of interest rates and possibly other variables intended to capture the stance of monetary policy.

that $i_t = ELB$, the shadow rate is a latent variable that can only take values below (or equal to) ELB, which will inform our inference about s_t. Before turning to our VAR-based specification of a process for s_t, we describe the conventional VAR approach.

2.1 Conventional VAR

A conventional VAR is a linear model for the evolution of a vector of observed data, y_t. Omitting intercepts, we have the following system of N_y equations for a VAR with p lags:

$$y_t = \sum_{j=1}^{p} A_j \, y_{t-j} + v_t \,, \qquad \text{with} \quad v_t \sim N(0, \Sigma_t). \tag{2}$$

Anticipating our subsequent application, we assume time-invariant transition matrices, A_j, but allow for time-varying shock volatilities, Σ_t, as in Clark (2011) and Carriero, Clark, and Marcellino (2019).[10] However, at this stage the system could also be represented more generally as a time-varying parameter VAR with stochastic volatility in the tradition of Cogley and Sargent (2005), Primiceri (2005), and Cogley, Primiceri, and Sargent (2010). Critically, VAR errors are typically assumed to have a symmetric distribution with unbounded support. When y_t includes the nominal interest rate, i_t, the resulting predictive densities will fail to incorporate the effects of the effective lower bound, with particularly detrimental effect when i_t is close to ELB. As a special case of (2), consider a random walk process for the nominal interest rate, $i_t = i_{t-1} + v_t$.[11] When $i_t = ELB$, the k-period-ahead point forecast still satisfies the ELB, since $E_t i_{t+k} = ELB$. But the associated density forecasts have 50 percent of their mass below ELB as the linear model ignores the ELB constraint.

[10] In our empirical application, we follow Carriero, Clark, and Marcellino (2019) and assume that $v_t = A_0^{-1} \Lambda_t^{-0.5} \varepsilon_t$, where A_0 is a lower unit-triangular matrix, Λ_t is a diagonal matrix, and the vector of its diagonal elements is denoted λ_t, with $\log \lambda_t = \log \lambda_{t-1} + \eta_t$, $\eta_t \sim N(0, \Phi)$, and $\varepsilon_t \sim N(0, I)$. Other forms of heteroskedasticity could also be specified.

[11] The random walk for i_t is a special case of the VAR in (2) with $y_t = i_t$, $p = 1$, $A_1 = 1$, and $A_j = 0$ $\forall \; i > 1$.

2.2 Truncated VAR

An applied fix to the ELB problem could be to estimate a standard VAR that ignores the ELB at the estimation stage, but then truncate the predictive densities for interest rates in the simulation stage. This approach is adopted by, for example, Schorfheide and Song (2020) in what they refer to as a poor man's version of the shadow-rate approach. We include this truncated VAR setup in our model evaluation.

When the ELB binds, the truncated VAR has a tendency to place substantial odds on a subsequent rise in i_t above the ELB. To see this, consider again the special case of a random-walk model for i_t. In this case, a forecast jump-off with $i_t = ELB$ leads to a heavily skewed predictive density that combines a point mass at ELB and a truncated normal distribution for values above the bound. At the one-step-ahead horizon, the odds of the nominal interest rate rising above the ELB are 50 percent (and increasing for longer horizons).[12] The resulting tendency to expect an imminent departure from the ELB contrasts with the shadow-rate VAR that is described next. In the basic version of the shadow-rate approach, the VAR vector includes the shadow rate, s_t, instead of the actual interest rate, i_t, and with $s_t < ELB$, predictions of future interest rates will need to see projections of s_t rise above the ELB to expect the same for i_t.

2.3 Shadow-rate VAR

The shadow-rate approach does not posit a VAR for the vector of observed variables, y_t, which contains the actual interest rate, i_t. Instead, a VAR is posited for a hypothetical data vector, z_t, that is identical to y_t except for replacing i_t with s_t. Without loss of generality, partition y_t in a vector of $N_x = N_y - N_s$ other variables, x_t, that have unbounded support,

[12] While the probability of $s_{t+k} > ELB$ remains at 50 percent at all horizons $k > 0$, the odds of $i_{t+k} > ELB$ are increasing with k, as the truncation $i_{t+i} = \max(s_{t+i}, ELB)$ is imposed at every step $i = 1, 2, \ldots, k$.

and the nominal interest rate i_t with x_t ordered on top:

$$y_t = \begin{bmatrix} x_t \\ i_t \end{bmatrix} \quad \text{and let} \quad z_t = \begin{bmatrix} x_t \\ s_t \end{bmatrix} \quad \text{with} \quad i_t = \max\left(ELB, s_t\right). \tag{3}$$

In the shadow-rate VAR approach we posit VAR dynamics for the partially latent vector z_t.[13] Analogously to (2) we have:

$$z_t = \sum_{j=1}^{p} A_j \, z_{t-j} + v_t \,, \qquad \text{with} \quad v_t \sim N(0, \Sigma_t). \tag{4}$$

The shadow-rate VAR system is a non-linear state space model that consists of the kinked measurement equation (3) and the linear state evolution described by the VAR in (4).[14]

Considering a standard VAR, Bernanke and Blinder (1992) proposed interpreting the policy rate equation of the VAR as a feedback rule that describes monetary policy.[15] In a similar spirit, the shadow-rate equation of the VAR model in (4) can be thought of as embedding a monetary policy reaction function that relates the shadow rate to the variables included in the VAR (4).[16] The actual policy rate follows the same reaction function, except that the actual rate is constrained to not fall below the ELB. As a result, the policy prescriptions from the model — evident in out-of-sample forecasts — obey the ELB on actual policy rates. In contrast, in a standard VAR ignoring the ELB, the implied reaction function relates the actual policy rate to the model's variables and allows the reaction function to prescribe a policy rate below the ELB.

Researchers might also be interested in allowing for potential time variation in parameters of the VAR. For example, in (4), VAR residuals have time-varying volatility. We leave

[13] The extension to higher-order systems is straightforward and described in Appendix A.

[14] In addition, the shadow-rate VAR system includes any state equations needed to track parameter drift, such as the time-varying volatilities embedded in Σ_t in the case of our application.

[15] The idea of capturing the systematic behavior of monetary policy by the policy rate equation of a VAR has spawned a rich literature, including Christiano, Eichenbaum, and Evans (1996, 1999), and Rotemberg and Woodford (1997).

[16] Using a smaller model in an unobserved components form, Johannsen and Mertens (2021) identify monetary policy shocks from surprises to the shadow rate, using short-run restrictions.

potential extensions to time variation in the VAR's regression coefficients, A_j, to future work. Identification of time-varying slope coefficients may become an issue since the shadow-rate components of z_t are latent when the ELB binds. Moreover, as noted by Mavroeidis (2020), the constant-parameter version of (4) is consistent with work by Swanson and Williams (2014), Debortoli, Gali, and Gambetti (2019), and Wu and Zhang (2019) that sees monetary policy as unconstrained by the ELB (for example, through the use of unconventional policies) so that economic dynamics remain unaffected by the ELB.

In reduced form, our shadow-rate VAR corresponds to what Mavroeidis (2020) refers to as "censored SVAR (CSVAR)." The truncated VAR corresponds to the reduced form of a "kinked VAR" in the terminology of Mavroeidis (2020), which is also used by Aruoba, et al. (2021). However, as discussed above, our implementation of the truncated VAR consciously disregards the implications of censoring for estimation of the VAR parameters, while the shadow-rate VAR explicitly includes interest rate censoring.

2.4 Estimation and forecasting

Each of our models is estimated with an MCMC sampler, based on the methods of Carriero, Clark, and Marcellino (2019) for large BVAR-SV models, with details provided therein. As in their work, we use a Minnesota prior for the VAR coefficients A_j and follow their other choices for priors as far as applicable, too.[17] Throughout, we use $p = 12$ lags in a monthly data set, which is described in further detail in Section 3. Here we briefly explain the algorithm adjustments needed to handle the shadow rate as a latent process whose posterior is truncated *from above* when the ELB binds.

Provided that data on s_t and thus z_t were always observed, estimation of the shadow-

[17] All VAR coefficients, A_j, have independent normal priors; all are centered around means of zero, except for the first-order own lags of certain variables as listed in Table 1. As usual, different degrees of shrinkage are applied to own- and cross-lag coefficients. Prior variances of the jth-order own lag are set to θ_1/j^{θ_4}. The cross-lag of the coefficient on variable m in equation n has prior variance equal to $\theta_1/j^{\theta_4} \cdot \theta_2 \cdot \hat{\sigma}_n^2/\hat{\sigma}_m^2$. The intercept of equation n has prior variance $\theta_3 \cdot \hat{\sigma}_n^2$. In all of these settings, $\hat{\sigma}_n^2$ is the OLS estimate of the residual variance of variable n in an AR(1) estimated over the entire sample. The shrinkage parameters are $\theta_1 = 0.05$, $\theta_2 = 0.5$, $\theta_3 = 100$, $\theta_4 = 2$, and $\theta_5 = 1$.

rate VAR in (4) would be straightforward to do with existing Bayesian MCMC methods for VARs.[18] However, when the data include observations for which the ELB is binding, not only does s_t become a latent variable, but it is also subject to the constraint that $s_t \leq ELB$ when $i_t = ELB$.

The shadow-rate VAR system consisting of (3) and (4) belongs to a class of conditionally Gaussian unobserved components models, for which Johannsen and Mertens (2021) have derived a generic shadow-rate sampling approach that can be nested inside an otherwise standard MCMC sampler for the VAR estimation. The Johannsen-Mertens approach employs the conditionally linear, Gaussian structure of the model to derive a truncated normal posterior for the vector of unobserved shadow rates in the system, given draws of other model parameters, such as the VAR coefficients A_j, and the stochastic volatilities captured by Σ_t.[19] Crucially, this truncated normal posterior pertains to the entire trajectory of unobserved shadow rates (or the ensemble of trajectories in the case of multiple ELB periods), necessitating draws from a multivariate truncated normal. Johannsen and Mertens (2021) successfully employ rejection sampling to generate joint draws from this multivariate shadow-rate posterior. However, in more general applications, rejection sampling can become computationally tedious and highly inefficient.[20]

Specifically, consider the following setup for the shadow-rate VAR given by (3) and (4): Values for the VAR coefficients $\{A_j\}_{j=1}^{p}$ and error variances $\{\Sigma_t\}_{t=1}^{T}$ are given and the data for $\{x_t\}_{t=1}^{T}$ are known. We further assume that at $t = 1$, p lags of the data for x_t are known,

[18] General textbook treatment is provided in, for example, Koop (2003) and Canova (2007). For the case of a medium-scale system with stochastic volatilities in the VAR residuals, as used in our application described further below, efficient methods are described by Carriero, Clark, and Marcellino (2019).

[19] For the remainder of this section, references to the shadow-rate posterior are understood as pointing to the posterior distribution of shadow rates conditional on other model parameters and other latent states, such as the sequence of the time-varying variance of covariance matrices for the residuals, $\{\Sigma_t\}_{t=1}^{T}$.

[20] For example, in an application like ours with monthly data for the US covering the years 2009 through 2015, the shadow-rate posterior is a multivariate truncated normal with (at least) 72 elements, necessitating a rejection whenever a single element out of these 72 should lie above the ELB. For illustrative purposes, consider the case where the shadow rate draws were *iid* with an individual probability of being below ELB of $\pi = 0.95$. The probability of all 72 draws lying below the ELB is then merely $0.95^{72} = 0.02$. Of course, in reality, we can expect positive serial correlation among adjacent shadow rates, but not every element's probability of falling below the ELB need be as high as 0.95, either.

and that the initial p lags of the shadow-rate vector, s_0, s_{-1}, ..., s_{-p+1}, are known.[21]

The shadow-rate s_t is unknown at least for some t.[22] For ease of notation, we normalize time subscripts so that the first time the ELB is binding occurs at $t = 1$. In addition, denote the last ELB observation by $T^* \leq T$ (where T is the length of the data sample), so that s_t is unknown for $1 \leq t \leq T^*$.[23] For simplicity we refer to the entire sequence $\{s_t\}_{t=1}^{T^*}$ as "unobserved," which corresponds to the case of a single ELB episode. However, the procedures described below also apply when multiple ELB episodes occur between $t = 1$ and T^*, so that only some, but not all, values of s_t in this window are unobserved. In addition, we define the vector $\bar{y}_t$ that contains the observed data except for observations of the actual interest rate at the ELB; we have $\bar{y}_t = x_t$ when the ELB is binding, and $\bar{y}_t = [x_t' \, s_t']'$ otherwise. As noted above, the vector of all observed variables is y_t.

For ease of reference, we collect all unobserved shadow rates in a vector $\boldsymbol{S}$ and all observations of $\bar{y}_t$ in a vector $\bar{\boldsymbol{Y}}$, and observations of y_t in a vector $\boldsymbol{Y}$:[24]

$$\boldsymbol{S} = \begin{bmatrix} s_{T^*} \\ s_{T^*-1} \\ \vdots \\ s_2 \\ s_1 \end{bmatrix}, \quad \text{and} \quad \bar{\boldsymbol{Y}} = \begin{bmatrix} \bar{y}_T \\ \bar{y}_{T-1} \\ \vdots \\ \bar{y}_0 \\ \bar{y}_{-p+1} \end{bmatrix}, \quad \text{and} \quad \boldsymbol{Y} = \begin{bmatrix} y_T \\ y_{T-1} \\ \vdots \\ y_0 \\ y_{-p+1} \end{bmatrix}. \tag{5}$$

The task of the shadow-rate sampler is then to sample $\boldsymbol{S} \,|\, \boldsymbol{Y}$, which includes the information that $\boldsymbol{S} \leq ELB$ (where the inequality is element-wise). Following Johannsen and Mertens (2021), the shadow-rate sampler builds on solving the "missing value" problem of characterizing $\boldsymbol{S} \,|\, \bar{\boldsymbol{Y}}$. The missing-value problem does not condition on information that the ELB

[21] Assuming that the ELB has not been binding for $t < 1$, we have observations on $s_t = i_t$ for $t = 0, -1, \ldots, -p+1$.

[22] Recall that the shadow rate is known (and identical to the actual rate) when $i_t > ELB$.

[23] Using more general notation, we could denote the time index of the first observation with a binding ELB by $T_0 + 1$, and consider the setup laid out here as normalizing the time index at $T_0 = 0$.

[24] The vector $\boldsymbol{S}$ is intended to capture only *unobserved* shadow rates. In the case of a single ELB episode lasting from $t = 1$ through T^*, $\boldsymbol{S}$ consists of the entire sequence $\{s_t\}_{t=1}^{T^*}$. In the case of multiple ELB episodes, observations where $s_t = i_t > ELB$ are excluded from entering $\boldsymbol{S}$.

has been binding for certain observations, and thus does not impose $\boldsymbol{S} \leq ELB$. As shown in Johannsen and Mertens (2021), the linear structure of the model and its Gaussian error distribution results in a posterior of the missing-value problem that is a multivariate normal, with the solution of the shadow-rate sampler being given by a corresponding truncated multivariate normal:[25]

$$\boldsymbol{S} \,|\, \bar{\boldsymbol{Y}} \sim N\left(\boldsymbol{\mu}, \boldsymbol{\Omega}\right) \tag{6}$$

$$\Rightarrow \quad \boldsymbol{S} \,|\, \boldsymbol{Y} \sim TN\left(\boldsymbol{\mu}, \boldsymbol{\Omega}, -\infty, ELB\right) . \tag{7}$$

The moments $\boldsymbol{\mu}$ and $\boldsymbol{\Omega}$ can be recursively computed using a standard Kalman smoother, and draws can be generated via a corresponding smoothing sampler.[26] Our paper extends the Johannsen-Mertens approach to a generic VAR with details provided in Appendix A.

A further contribution of our paper is the implementation of the shadow-rate sampler via Gibbs sampling, following Geweke (1991), and adapted to the variance-covariance structure of the VAR(p) case, rather than the rejection sampling employed by Johannsen and Mertens (2021). Depending on parameter values, a (well-known) issue with rejection sampling from the truncated normal is a possibly low acceptance rate. In our case, the acceptance probability in sampling from (7) critically depends on VAR parameters and the observed data for macroeconomic and financial variables (other than the federal funds rate). As reported further below, when VAR parameters are drawn from the eventual posterior of our shadow-rate VAR, the acceptance probability that draws from the missing-value problem will lie below the ELB is fairly high. However, this need not be the case in general, and does not hold, for example, when our VAR is estimated while treating observations for the federal funds rate as missing (rather than censored) data when the ELB binds. Our adaptation of the

[25] The notation $\boldsymbol{S} \sim TN(\boldsymbol{\mu}, \boldsymbol{\Omega}, a, b)$ denotes a truncated multivariate normal distribution for the random vector $\boldsymbol{S}$, with typical elements s_j, where $a \leq s_j \leq b \; \forall \, j$, and where $\boldsymbol{\mu}$ and $\boldsymbol{\Omega}$ are the mean vector and variance-covariance matrix of the underlying normal distribution.

[26] Alternatively, the moments $\boldsymbol{\mu}$ and $\boldsymbol{\Omega}$ could be computed using the sparse methods of Chan and Jeliazkov (2009).

Gibbs sampling approach of Geweke (1991) to the VAR(p) case, with details described in Appendix A, provides a more efficient solution to the shadow-rate sampling problem.

In out-of-sample forecasting, for every model considered (standard/truncated/shadow rate), we simulate draws from the predictive density of y_{t+k} at forecast origin t by recursive simulations. In each case, to generate draws from the h-step-ahead density, VAR residuals, v_{t+k}, are drawn for $k = 1, 2 \ldots, h$.[27] In the case of the standard VAR, conditional on current and lagged data for y_t, the simulation is standard and iterates over (2). For the truncated VAR, the iteration also proceeds using (2), but applies the censoring function (1) to predictions for interest rates at every step of the forecast simulation.[28] In contrast, for the shadow-rate VAR, simulation of the predictive densities jumps off MCMC draws for s_t, s_{t-1}, $\ldots s_{t-p+1}$ that are used to initialize recursions over (4). In the case of the baseline shadow-rate VAR, censoring of predicted interest rates is applied only at the level of the measurement equation (1), while uncensored draws of lagged shadow rates are fed into the VAR equation (4) to simulate subsequent predictions of y_{t+k}.

3 Data

Our data set consists of monthly observations for 18 macroeconomic and financial variables for the sample 1959:03 to 2020:09, taken from the October 2020 vintage of the FRED-MD database maintained by the Federal Reserve Bank of St. Louis. The variables and their transformations to logs or log-differences are listed in Table 1. Reflecting the raw sample, transformations, and lag specification, the sample for model estimation always begins with 1960:04. Critically, the data set includes the federal funds rate, which was constrained by the ELB from late 2008 through late 2015, and has been again starting in March 2020.

[27] As described in, for example, Carriero, Clark, and Marcellino (2019), draws from $v_{t+k} \sim N(0, \Sigma_{t+k})$ are conditioned on an MCMC draw of the underlying model parameters and SV states and involve forward simulation of the SV processes.

[28] In our application, there are three interest rate variables: the federal funds rate, plus nominal yields on 5- and 10-year Treasury bonds. Censoring is applied to predictions of all three of them in the case of the truncated VAR as well as the shadow-rate VAR.

In addition to the federal funds rate, our data set contains two longer-term interest rates, measuring the yields on Treasury bonds with maturities of 5 and 10 years. Data for the federal funds rate and these two longer-term yields are shown in Figure 1. During and following the Great Recession, longer-term bond yields remained solidly or well above the ELB. The 10-year (5-year) Treasury yield declined from 2.4 percent (1.5 percent) in December 2008 to a low of 1.5 percent (0.6 percent) in July 2012 and then moved higher. Since the COVID-19 outbreak and the FOMC's quick and substantial easing of monetary policy, bond yields have been lower than they were following the Great Recession and much closer to the ELB. From April through September 2020, the 10-year (5-year) Treasury yield averaged 0.7 percent (0.3 percent).

In our application with US postwar data, the value of ELB is set to 25 basis points, which was the upper end of the FOMC's target range for the federal funds rate between late 2008 and 2015, and has been again since the spring of 2020.[29] As a matter of consistency with this convention, we set readings for the federal funds rate to 25 basis points when estimating the shadow-rate VAR (not when including the federal funds rate in a standard VAR that ignores the lower bound constraint). Yields with maturities of five years and longer stayed above 25 basis points in the data and can thus be treated as part of the vector x_t, defined in Section 2, for the purpose of model estimation.[30]

4 Shadow-rate estimates

Figure 2 reports our shadow-rate estimates associated with the federal funds rate, along with a comparison to measures from Krippner (2013, 2015) and Wu and Xia (2016) based on affine term structure models. Panel (a) of the figure compares full-sample estimates using data through September 2020 (black/red line with the credible set indicated by gray shading) to

[29] See, for example, Wu and Xia (2016) and Johannsen and Mertens (2021).

[30] The lower bound constraint is an issue when simulating the predictive density for these yields, but it is not relevant for estimating the VAR.

quasi-real-time estimates (solid red line with the credible set indicated by dotted lines).[31] The quasi-real-time estimates are the end-of-sample estimates produced by recursive estimation of the model starting in January 2009. Panel (b) compares our full-sample estimate to the Krippner and Wu-Xia measures.

The full-sample estimates show the shadow rate dropping sharply starting in 2009, reaching a nadir of about -1.7 percent in late 2011. The rate then gradually rose and reached the ELB in early 2016, following the Federal Reserve's first increase in the federal funds rate in December 2015 (when the FOMC raised the target range from 0-25 basis points to 25-50 basis points). The rate dropped precipitously in early 2020, with the posterior median reaching about -90 basis points in May 2020, and hovered near that level through the end of our sample in September 2020. As might be expected, the quasi-real-time estimates have more time variability than do the full sample estimates, but follow a quite similar contour. As might also be expected, the quasi-real-time estimates are less precise, with credible sets wider than those of the full sample estimate (more so for the 2009-2015 period than 2020, as might be expected, given that, at this time, little history is available on the current ELB episode).

Although our VAR does not impose the restrictions of an affine term structure model, our shadow-rate estimates have some similarities to the Krippner and Wu-Xia measures based on affine term structure models. As indicated in Panel (b) of Figure 2, our estimate and the Wu-Xia series move together from 2009 through 2013. But over the remainder of the ELB episode following the Great Recession, as our estimate gradually rose to the ELB over the course of 2014 and 2015, the Wu-Xia series fell and then rose sharply. Our estimate also follows the same general contours as the Krippner measure, although the Krippner series shows much sharper declines.

Figure 3 provides some comparisons to assess the effects of shadow-rate modeling and enforcement of the ELB in model estimation. Panel (a) compares shadow-rate (black) and

[31] To be clear, in the full sample case, the model is estimated with data for 1960:04 through 2020:09, but the figure omits the period of 1960-2008 during which the ELB did not bind.

missing-data (red) draws for the shadow rate s_t obtained from the posterior of our baseline shadow-rate VAR. Shadow-rate draws are obtained from the truncated posterior for s_t that satisfies the ELB, and described by the problem of drawing from $\boldsymbol{S}|\boldsymbol{Y}$ in (7). Missing-data draws are obtained from the underlying (and untruncated) posterior of the missing data problem, which ignores the ELB, and correspond to draws from $\boldsymbol{S}|\bar{\boldsymbol{Y}}$ in (6). For much of the sample, the posteriors obtained from these alternatives are very similar.[32]

These results might suggest that an approach that treats observed policy rates at the ELB as missing values might be a close alternative to shadow-rate sampling that explicitly accounts for the ELB.[33] However, such a conclusion would neglect the effects of enforcing the ELB as part of the shadow-rate sampling on inference for other VAR parameters and state variables (like SV). As discussed by Waggoner and Zha (1999) in the context of conditional forecasting, conditioning estimates on information when the ELB was binding could (and should) embody non-trivial information about the relevant parameters of the VAR.

To illustrate these effects, Panel (b) compares missing-data posteriors obtained from two sets of VAR estimates: In the baseline (red), parameter and SV draws reflect shadow-rate sampling (as shown also in Panel (a)). In the alternative version (blue), parameters and SV are drawn while treating the policy rate at the ELB as missing data and without requiring that missing data draws lie below the ELB. The comparison highlights the non-negligible effects of shadow-rate sampling, which takes into account observations of interest rates at the ELB, on model estimates of parameters and SV. Without forcing the draws of missing interest rate observations to lie at or below the ELB, the upper bound of the posterior credible set rises sharply above the ELB for much of the 2009-2011 period and again in 2020, which contradicts observations of the federal funds rate that were at the ELB during those times. In contrast, the use of shadow-rate sampling, as opposed to a missing-data approach, leads to estimates of parameters and SV that increase the odds of obtaining missing-data

[32]Early in the Great Recession episode and in the early months of the COVID-19 episode, using a missing data approach without fully enforcing the ELB led to draws of interest rates above the ELB, whereas with the full shadow-rate treatment, the interest rate distributions remained at or below 25 basis points.

[33]Such a missing data approach has been used by, for example, Del Negro, et al. (2017).

draws for the shadow rate that lies below the ELB (for observations when the ELB binds).

5 Forecast evaluation

We conduct an out-of-sample forecast evaluation in quasi-real time, where we simulate forecasts made from January 2009 through September 2020. For every forecast origin, each model is re-estimated based on growing samples of data that start in 1959:03. (As indicated in tables provided in the supplementary appendix, we obtain very similar results when we shorten the sample to end in December 2017 to avoid the unusual volatility of the COVID-19 pandemic).[34] Of course, in either case the evaluation window is relatively short and largely informed by a single ELB episode. Forecasts made prior to 2009 are not considered, due to the absence of observed interest rates at the ELB in postwar US data. All data are taken from the October 2020 vintage of FRED-MD; we abstract from issues related to real-time data collection.

5.1 Average performance 2009–2020

Tables 2, 3, and 4 provide results on point and density forecast accuracy, measured by root mean squared error (RMSE, computed around mean forecasts), mean absolute error (MAE, computed around median forecasts), and continuous ranked probability score (CRPS), respectively.[35] The reported forecast horizons are $h = 3$, 6, 12, and 24 months.

To facilitate comparisons, we report RMSE, MAE, and CRPS results as relative to the baseline of a standard VAR that simply takes the forecasts as given and does nothing to obey ELB constraints, so that entries of less (more) than 1 mean a given forecast is more (less)

[34] In companion work we investigate the use of outlier-adjusted versions of the SV model to handle the particular swings in data seen since the outbreak of COVID-19 (Carriero, et al., 2021). Through the use of latent states to capture outliers, the outlier-adjusted procedures discussed there retain a conditionally Gaussian representation, and combination with the shadow-rate sampling methods described here is straightforward. For the sake of parsimony, we maintain a standard SV specification in the present paper, which should, however, not materially affect the relative comparisons shown here.

[35] The online appendix also reports median absolute deviations (MAD) around median forecasts.

accurate than the baseline. To roughly gauge the significance of differences with respect to the baseline, we use t-tests as in Diebold and Mariano (1995) and West (1996), denoting significance in the tables with asterisks. In light of the concerns of Bauer and Rudebusch (2016) with the use of mean forecasts for interest rates near the ELB constraint, we also report results for median forecasts evaluated with a mean absolute error loss function (MAE). Measured by MAE, the performance of median forecasts is qualitatively similar to the RMSE performance of the corresponding mean predictions. However, quantitatively, the gains from applying the shadow-rate VAR are even more substantial in the case of interest rates.

As a starting point, consider the simplest possible approach to obeying the constraints of the ELB: simply truncating interest rate forecasts to rule out values below the ELB. As indicated in columns 2-5 of the tables, this simple approach is helpful in one respect but harmful or of little consequence in others. In particular, the truncated specification materially improves federal funds rate forecasts, with RMSE, MAE, and CRPS ratios of roughly 0.5 to 0.8 for $h = 3$, 6, 12, and 24 (except for a relative RMSE near 1 for h=24). But the truncated approach harms the accuracy of forecasts of Treasury bond yields at horizons of 6 months and more. For example, with $h = 12$, the RMSE, MAE, and CRPS ratios for the 10-year Treasury yield are 1.34, 1.29 and 1.24, respectively. For indicators of economic activity, measures of inflation, and other financial indicators, the truncated approach has little consistent effect on accuracy. In a few cases, the truncated approach yields forecasts more accurate than the standard VAR baseline (e.g., for PCE inflation), whereas in some others, the truncated forecasts are less accurate than the baseline (e.g., the unemployment rate).

Our proposed shadow-rate specification for accommodating the ELB performs better in forecasting than does simple truncation. Results for these specifications are covered in columns 10-13 of Tables 2, 3, and 4. Compared to the standard VAR baseline, the shadow-rate specification significantly improves forecasts of not only the federal funds rate (FFR) but also bond yields, without harming the forecasts of indicators of economic activity, measures

of inflation, and other financial indicators. With our preferred approach to accommodating the ELB, RMSE ratios for FFR forecasts for $h = 3$, 6, 12, and 24 range from 0.34 to 0.52, the MAE ratios range from 0.26 to 0.35, and the CRPS ratios range from 0.28 to 0.34, with statistical significance of all of the MAE and CRPS gains.[36] The funds rate forecasts from the shadow-rate specification are more accurate than those from the truncated specification. In addition, unlike the approach based on truncation, the shadow-rate VAR improves forecasts of 5- and 10-year Treasury yields, more so at longer horizons than at shorter horizons. For example, the shadow-rate model's RMSE ratios for the 5-year yield decline from 0.93 at h=3 to 0.70 at h=24, with very similar results of density forecast accuracy as measured by the CRPS. In the case of the Baa-Treasury spread, the shadow-rate specification performs much better than the truncated specification, and its forecasts are quite a bit more accurate than those obtained from the standard VAR for $h = 6$, 12, and 24 (and on par for $h = 3$). Finally, for the indicators of economic activity, stock price returns, and the exchange rate, the treatment of the ELB on interest rates does not seem to bear consistently and importantly on forecast accuracy. RMSE, MAE, and CRPS ratios for the truncated and shadow-rate specifications are often close to 1. In fact, to take real consumption and non-farm payrolls as examples, the RMSE ratios are all 1.00 (for each of four forecast horizons and three specifications). In some cases, our preferred shadow-rate specification yields forecasts a little more accurate than the standard VAR (e.g., 24-months-ahead point forecasts for hourly earnings). This specification also tends to improve forecasts of housing starts, perhaps the most interest-rate-sensitive activity indicator in the model. In a few cases, our preferred forecasts are somewhat less accurate than the baseline (e.g., 24-months-ahead forecasts for capacity utilization).

In addition, we compare point and density forecasts from our preferred shadow-rate VAR against those obtained from a plug-in approach, where external shadow-rate estimates,

[36] As reported in the online appendix, gains for median absolute deviations around the median predictions (MAD) from the shadow-rate VAR are even maximal, since the median forecasts for the reported horizons correctly predict the FFR outcome for at least half the times during our evaluation window, leading to perfect MAD scores of 0.

specifically from Krippner (2013, 2015) and Wu and Xia (2016), are used as data, in place of the actual short-term interest rate, in an otherwise standard VAR. Following the spirit of the shadow-rate literature, and different from the truncated VAR discussed before, forecasts from the plug-in VAR are simulated without censoring the resulting (shadow) interest rate projections. Similar to the case of our shadow-rate VAR, forecasts for nominal interest rates are censored only after the dynamic simulations for all variables (and all horizons) have been done. As reported in Tables 5 and 6, we find consistent benefits for point and density forecasting from using the shadow-rate VAR across a wide range of variables. Note that the forecasts obtained from the plug-in VAR are based on the latest vintages of full-sample estimates for the shadow rates from Krippner and Wu-Xia. Since these shadow-rate estimates abstract from one-sided filtering challenges (and other revisions), the results reported in Tables 5 and 6 likely understate the gains that could be achieved in (quasi-)real-time forecasting from our preferred shadow-rate VAR when compared to a plug-in approach.

In addition, our online appendix reports various robustness checks, with fairly similar results to what is reported here. In particular, in light of concerns raised by Krippner (2020), we replace various interest rates with alternative measures of similar maturities. Replacing the 10-year Treasury yield, as used in our baseline, with the 20-year Treasury yield has little effect on our results. Using the 3-month Treasury bill rate, instead of the federal funds rate, also delivers broadly similar forecast comparisons; if anything, these T-bill results favor the shadow-rate VAR a little more than what is reported here for the funds-rate-based specification. We also consider alternative versions of the truncated and shadow-rate VAR based on setting the ELB to 12.5 basis points (rather than 25 basis points). While the ELB tends to bind a little less often in this case, the forecast comparisons tend to display similar patterns as in our baseline results. Finally, the online appendix reports alternative forecast comparisons, derived from a slightly shorter evaluation period, ending in 2017:12, to avoid having data related to the outbreak of the COVID-19 pandemic in 2020 affect the results. While the economic effects of the pandemic left a heavy mark on readings of macroeconomic

and financial variables in 2020 — see, for example, our companion work in Carriero, et al. (2021) — they did not materially affect the relative model forecast comparisons reported here.

5.2 Interest rate forecasts made at selected origins since 2009

To this point, the results presented have focused on the average performance of the various models over the entire evaluation sample. In broad terms, these comparisons show that our proposed shadow-rate specification performs best for forecasting the federal funds rate, with the truncated approach not quite as good, and the standard VAR materially worse. To get a better understanding of this relative performance, and also to get a glance at the absolute performance, it is instructive to compare the point and density forecasts of the federal funds rate for selected forecast origins. Figure 4 reports a set of point forecasts (medians) and 68 percent bands of distributions, at horizons of 1 through 24 months, in December of 2013, 2014, 2015 (when the FOMC raised the funds rate), 2016, and 2018. In this figure, the actual path of the federal funds rate is represented by green dots.

To illustrate the effects of ignoring the ELB, Panel (a) of Figure 4 compares forecasts from a standard VAR ignoring the ELB with forecasts from the truncation approach, using a forecast origin of 2013:12, two years before the FOMC actually raised the funds rate target from the ELB.[37] In this case, the point forecast from ignoring the ELB (solid red line) proves a little more accurate than the forecast obtained with the truncation approach (solid blue line), although this do-nothing point forecast is negative for the entire forecast horizon, in contrast with the ELB. The uncertainty around the do-nothing point forecast is also generally larger than for the truncated model, in particular at longer horizons.

The remaining panels of Figure 4 compare forecasts from the truncation approach (black line with gray shading) to those from our shadow-rate specification (blue lines), for forecast

[37]For brevity, our discussion will abstract from nuances of the real-time data flow, and simply refer to forecasts being "made" at (or even "in") the month of a particular forecast origin, even though the underlying data would have been available in FRED-MD only in a subsequent month.

origins in December 2013, 2014, 2015, 2016, and 2018. In the examples for the years before the FOMC raised the funds rate target above the ELB, the point forecasts from the shadow-rate specification are much more accurate than those from the model using truncation. The differences are clearly large in 2013, 2014, and 2015, when the shadow-rate forecast is at or just slightly above the ELB throughout the forecast horizon, whereas the truncation-based forecast rises throughout the horizon. Throughout most of our evaluation window, the median forecasts from the shadow-rate model correctly predict that the FFR will stay at the ELB. Moreover, considering forecasts made in 2013, 2014, and 2015, it is also striking that the forecast intervals are much narrower with the shadow-rate specification. Although the same basic patterns prevail in subsequent years, the specifics of the pictures evolve. In the case of forecasts made in 2015:12, both the shadow rate and the truncation approaches show increases in the funds rate, but the shadow rate's increase is later and much smaller than that projected by the truncated specification.

In the 2016:12 and 2018:12 cases, both coming after the FOMC had raised the funds rate off of the ELB, forecasts from the shadow rate and truncated specifications are relatively similar. In Panel (e), depicting forecasts made in 2016:12, both models underpredict the increase in the funds rate that eventually happens. Given the earlier behavior of the FFR, neither model had enough information to predict the sharp increase in the FFR that would have taken place in the following months. Finally, Panel (f) shows forecasts made in 2018:12 — with the forecast horizon extending out to 2020:12 — with the COVID-19 period included in the evaluation sample. Both specifications predict a decline in the funds rate over the first 9 months that was sharper than actually occurred, but starting in March 2020, the funds rate fell much faster than the models predicted. Of course, no model could have predicted — 15 months ahead — the outbreak of the pandemic and the easing of monetary policy that followed.

From a mechanical perspective, the tendency of the truncated VAR to place larger odds on interest rate increases near the ELB reflects its dependence on lagged actual rates, which are

censored, rather than the uncensored shadow rates, as discussed in Section 2. The impact of modeling interest rate (actual rates, not shadow rates) forecasts via the uncensored shadow-rate dynamics is illustrated in Figure 5. Panels (a) and (b) of the figure compare actual rate densities generated by the shadow-rate VAR (densities also shown in Panels (b) and (d) of Figure 4) for jump-off dates 2013:12 and 2015:12, against the underlying predictive densities of the shadow rate. Panels (c) and (d) depict predictive densities generated upon entry into the ELB periods beginning in 2009 and 2020. As shown in all panels of Figure 5, predictive densities for the shadow rate are highly persistent, reflecting the persistence of actual rates observed prior to the ELB data in our sample. As a result, when the shadow rate is seen to lie substantially below the ELB, expectations that the actual rate will depart from the ELB are pushed out substantially.

From an economic perspective, the shadow-rate VAR can capture lower-for-longer or make-up elements of the Federal Reserve's monetary policy strategy through the dependence of predicted interest rates on lagged notional rates as suggested by, for example, the models of Reifschneider and Williams (2000), Gust, et al. (2017) and Billi (2020). Moreover, the shadow-rate estimates are informed by observed data on longer-term yields and economic conditions, which enables the estimates to pick up on the effects of unconventional policies, such as forward guidance and asset purchases, through these channels.

5.3 Forecasts made since the outbreak of COVID-19 in 2020

The period following the outbreak of the COVID-19 pandemic in the US and the aggressive easing of monetary policy by the FOMC provides an opportunity for a case study of predicted interest rate dynamics from our shadow-rate VAR as compared to a standard VAR that ignores the ELB and a VAR approach that relies on truncation. Figure 6 shows the evolution of federal funds rate forecasts over selected origins between January and September 2020. In January 2020, prior to the outbreak of COVID-19 in the US, forecasts from all model variants could, of course, not yet foresee the outbreak of COVID-19, and predicted the FFR

to hover around its then-value of about 1.5 percent for the next two years.[38] Once the outbreak of COVID-19 hit the US economy, in March and April, the point forecast from a standard VAR puts the funds rate well below the ELB for the entire forecast horizon, with substantial probability mass on very negative rates. At subsequent forecast origins, the point forecast was close to the ELB, but substantial mass in the predictive distribution remained in negative territory. At the other extreme, the approach of truncating federal funds rate predictions at the ELB resulted in point forecasts that had the federal funds rate gradually rising over the forecast horizon, with substantial probability mass on quite high rates. These results reflect the dependence of predicted values in the truncated VAR on lagged actual rates, which are censored, rather than the uncensored shadow rates.

Through the first half of the year, the point forecast of the funds rate from the shadow-rate approach remained at the ELB throughout the forecast horizon. In later months, the point forecast from the shadow-rate VAR shows a small increase in the funds rate after 12 months or so. In all cases, the predictive distributions from the shadow-rate VAR are considerably narrower than those obtained with the truncation approach.

Forecasts of the federal funds rate from the shadow-rate VARs reflect the predicted evolution of the shadow rate (not shown in the interest of chart readability). As noted before, shadow rates reflect the unconstrained policy rate prescriptions of the feedback rule for monetary policy that is implied by the VAR in (4).[39] As a reference point, the Federal Reserve Bank of Cleveland regularly publishes a set of policy path prescriptions obtained from monetary policy rules in the tradition of Taylor (1993, 1999). Prescriptions are derived from seven different rules and for three alternative sets of forecasts for economic conditions; similar to our shadow-rate concept, all prescriptions ignore the ELB.[40] Some of these rules

[38]Nevertheless, uncertainty bands generated from the standard VAR assigned odds of over 30 percent to the event of the funds rate falling below the ELB after a year and a half.

[39]The interpretation of the shadow-rate VAR as embedding the monetary feedback rule for the federal funds rate extends arguments made by, for example, Bernanke and Blinder (1992), Christiano, Eichenbaum, and Evans (1996, 1999), and Rotemberg and Woodford (1997) in the context of a standard VAR to the shadow-rate case.

[40]The rule results and documentation are available at `https://www.clevelandfed.org/en/our-research/indicators-and-data/simple-monetary-policy-rules.aspx`. Prescriptions from a sim-

are so-called "inertial" rules that generate prescriptions with strong lagged dependence on past policy rates. At the ELB, inertia with respect to lagged unconstrained prescriptions (or so-called notional rates) can capture lower-for-longer policies as discussed by, for example, Billi (2020), and resemble the form of the feedback rule embedded in our shadow-rate VAR.

With data available as of December 1, 2020, the median rule prescription calculated by the Federal Reserve Bank of Cleveland puts the federal funds rate at about −50 basis points in 2020:Q4 and −70 basis points for the first three quarters of 2021. In comparison, our shadow-rate estimates for the COVID-19 period from April through September 2020 are modestly negative (about −40 basis points in September 2020), which broadly aligns with unconstrained prescriptions of common policy rules.[41] Moreover, the shallow funds-rate path predicted by the shadow-rate VAR is also much closer to survey expectations obtained from Blue Chip Financial Forecasts and the Survey of Professional Forecasters (SPF).[42]

6 Conclusion

Motivated by the prevalence of lower bound constraints on nominal interest rates, this paper develops a tractable approach to including a shadow-rate specification in medium-scale VARs commonly used in macroeconomic forecasting. Our model treats interest rates as censored observations of a latent shadow-rate process in an otherwise standard VAR setup, with the shadow rate allowed to go below the ELB when the actual interest rate is at the ELB, and with the shadow rate equal to the observed interest rate when the ELB is not binding. Our approach extends the specific unobserved components model of Johannsen and Mertens (2021) to the general VAR setting. By using a computationally more efficient shadow-

ilar set of policy rules are also computed by staff at the Board of Governors and presented to the FOMC ahead of each of its meetings as part of Tealbook Book B; see also Board of Governors of the Federal Reserve System (2020).

[41] We refer to rule prescriptions that ignore the ELB on the federal funds rate as "unconstrained."

[42] For example, the 2020:Q3 SPF does not see any significant rise in the 3-month Treasury rate before the end of 2023, which is an even shallower path than the funds-rate projections from the shadow-rate VAR shown in Panel (e) of Figure 6 for September 2020. The 2021:Q1 SPF sees a modest rise in short-term interest rates over the course of 2023.

rate sampling algorithm than Johannsen and Mertens (2021), together with the recursive methods of Carriero, Clark, and Marcellino (2019) for efficient estimation of Bayesian VARs with stochastic volatility, our approach is easily applied to a medium-scale VAR system.

We use our shadow-rate approach to form forecasts from a medium-scale BVAR with stochastic volatility. In our results, forecasts for interest rates obtained from a shadow-rate VAR for the US since 2009 are clearly superior, in terms of both point and density forecasts, to predictions from a standard VAR that ignores the ELB. These interest rates include not only the federal funds rate but also longer-term bond yields. For other indicators of financial conditions and measures of economic activity and inflation, the accuracy of forecasts from our shadow-rate specification is broadly on par with a standard VAR that ignores the ELB. Overall, our shadow-rate specification successfully addresses the ELB and improves interest rate forecasts without harming a standard VAR's ability to forecast a range of other variables.

A Shadow-rate sampling

This appendix provides further details on the application of a shadow-rate sampler in a VAR context that can be embedded in an otherwise standard MCMC estimation. Throughout, we take as given values of all parameters (incl. SV) of the shadow-rate VAR in (4). These parameter values can be obtained from standard MCMC steps (and based on previously sampled "data" for $\{z_t\}_{t=1}^T$) as described in, for example, Carriero, Clark, and Marcellino (2019)). Here we focus on the MCMC step concerned with sampling from the shadow-rate problem stated in (7) for given values of the VAR parameters $\{A_j\}_{j=1}^p$ and $\{\Sigma_t\}_{t=1}^T$. For ease of notation, references to $\{A_j\}_{j=1}^p$ and $\{\Sigma_t\}_{t=1}^T$ will be suppressed from the conditioning sets described below. Moreover, the value of ELB is a known constant. For ease of exposition, we continue to focus on the case of a scalar shadow rate, s_t, which can, however, be easily generalized to the case of $N_s > 1$.

A.1 Gibbs sampling from the truncated multivariate normal

While the joint density from a multivariate normal (MVN) distribution can be factorized into a product of univariate normal densities, the same property does not generally extend to the truncated MVN density, as discussed by, for example, Geweke (1991). In our context, this means that draws from the missing-value problem, $\boldsymbol{S} \,|\, \bar{\boldsymbol{Y}} \sim N(\boldsymbol{\mu}, \boldsymbol{\Omega})$ in (6), could be recursively obtained by a sequence of univariate normal draws, but not so for the corresponding shadow-rate problem $\boldsymbol{S} \,|\, \boldsymbol{Y} \sim TN(\boldsymbol{\mu}, \boldsymbol{\Omega}, -\infty, ELB)$. However, consider a single element of $\boldsymbol{S}$, denoted s_t, and let $s_{1:t-1}$ and $s_{t+1:T}$ denote the vectors of all elements of $\boldsymbol{S}$ that precede and follow s_t, respectively.[43] Conditional on $s_{1:t-1}$ and $s_{t+1:T}$ (as well as $\boldsymbol{Y}$), s_t has a univariate truncated normal distribution,

$$s_t \,\big|\, s_{1:t-1}, s_{t+1:T}, \boldsymbol{Y} \sim TN\left(\mu_{1:t-1,t+1:T}, \omega_{1:t-1,t+1:T}, -\infty, ELB\right) , \tag{8}$$

with moment parameters $\mu_{1:t-1,t+1:T}$ and $\omega_{1:t-1,t+1:T}$ identical to those obtained from the corresponding missing-value problem:[44]

$$s_t \,\big|\, s_{1:t-1}, s_{t+1:T}, \bar{\boldsymbol{Y}} \sim N\left(\mu_{1:t-1,t+1:T}, \omega_{1:t-1,t+1:T}\right) . \tag{9}$$

As discussed by Geweke (1991), Gelfand, Smith, and Lee (1992), and references therein, the fact that conditional distributions of the truncated MVN are also truncated normals means that the problem of obtaining draws from the truncated MVN can be addressed with a Gibbs sampler, which we also pursue. For now, we abstract from estimating the VAR, and consider solely the shadow-rate sampling problem for given VAR parameters. Adopting

[43] In the case of $N_s > 1$, so that s_t is not scalar, the argument made here applies to a single scalar element of s_t conditional on values for the remainder of the shadow-rate vector, as well as $s_{1:t-1}$, $s_{t+1:T}$, and $\boldsymbol{Y}$.

[44] For recent treatments, see, for example, Horrace (2005) and Chopin (2011). The argument also extends to the case in which the truncation bounds vary from one element of the vector to another, which also allows us to handle where the sequence $s_{1:T}$ covers observations where the ELB does not bind, so that $s_t = i_t > ELB$. To handle those cases, the shadow-rate sampling problem can be stated more generally as $\boldsymbol{S} \,|\, \boldsymbol{Y} \sim TN(\boldsymbol{\mu}, \boldsymbol{\Omega}, -\infty, \boldsymbol{I})$, where $\boldsymbol{I}$ is the vector of all actual rates, and the inequality $\boldsymbol{S} \leq \boldsymbol{I}$ applies element-wise. Note that observations of i_t for which the ELB does not bind are included in $\bar{\boldsymbol{Y}}$ so that the distribution of the missing-value problem in (6) collapses on a point mass, $s_t = i_t$, for those observations.

language from Geweke (1991), a Gibbs sampler generates a draw from (7) by performing N passes over (8), at each pass iterating over $t = 1, 2, \ldots T$.[45] Specifically, let $\boldsymbol{S}^{(n)}$ denote a draw of $\boldsymbol{S}$ from the nth pass of the Gibbs sampler, with typical element $s_t^{(n)}$. At each pass $n = 1, 2, \ldots, N$, the Gibbs sampler iterates from $t = 1, 2 \ldots, T$ and draws

$$s_t^{(n)} \Big| \, s_{1:t-1}^{(n)}, s_{t+1:T}^{(n-1)}, \boldsymbol{Y} \tag{10}$$

We keep $\boldsymbol{S}^{(N)} = \{s_t^{(N)}\}_{t=1}^T$ as the draw from (7). Appendix A.4 describes in further detail how this Gibbs sampler for the shadow-rate problem is embedded in our MCMC sampler for the shadow-rate VAR.

Our implementation of the Gibbs sampling steps for the shadow-rate problem in (8) exploits the particular structure of the VAR(p) setting to derive the conditional moments $\mu_{1:t-1,t+1:T}$, $\omega_{1:t-1,t+1:T}$ without ever having to compute the entire mean vector, $\boldsymbol{\mu}$, and variance-covariance matrix, $\boldsymbol{\Omega}$, of the full shadow-rate problem in (7), which can be substantial in size because $\boldsymbol{S}$ is a vector of size $T \cdot N_s$.[46] For example, in our application to monthly US data, and considering only the ELB episode witnessed from 2008:12 through 2015:12, we have $T = 85$ and $N_s = 1$ (as the ELB has only been binding for the federal funds rate in our data set over this period).

In the case of $N_s = 1$, drawing from (8) requires a draw from the (univariate) truncated normal distribution.[47] We implement this draw by application of uniform-inverse-transform sampling as follows. Dropping time subscripts, consider the problem of drawing the scalar $s \sim TN(\mu, \omega^2, -\infty, ELB)$, which is equivalent to drawing $v \sim TN(0, 1, -\infty, \bar{v})$ with $\bar{v} =$

[45] When the sequence $s_{1:T}$ includes observations t where the ELB does not bind, the posterior in (9) collapses on a point mass, $s_t = i_t > ELB$, and those cases can be skipped. (Formally, the support of the truncated normal in (8) could be viewed as being bounded from above by i_t for all observations t.)

[46] By exploiting sparsities and the recursive structure of the VAR's state space representation, our approach echoes recent advances in the field of sampling from the truncated MVN distribution made by Cong, Chen, and Zhou (2017), albeit specialized to the VAR(p) that we intend to investigate further. Other advances in Gibbs sampling from the truncated MVN distribution are discussed by Robert (1995), Damien and Walker (2001), Chopin (2011), and Botev (2017).

[47] In the case of $N_s > 1$, (8) represents a draw from the multivariate truncated normal, which can be broken down further into a sequence of Gibbs sampling steps consisting of draws of univariate truncated normals, as described by, for example, Geweke (1991).

$(ELB - \mu)/\sigma$ and $s = \mu + \sigma\, v$. The support of v is $v \leq \bar{v}$, over which its probability density function (*pdf*) and cumulative distribution function (*cdf*), $f_v(v)$ and $F_v(v)$, are given by:

$$f_v(v) = \frac{\phi(v)}{\Phi(\bar{v})}\,, \qquad\qquad F_v(v) = \frac{\Phi(v)}{\Phi(\bar{v})}, \tag{11}$$

where $\phi(\cdot)$ and $\Phi(\cdot)$ are the standard normal *pdf* and *cdf*, respectively, and draw

$$u \sim U(0,1) \qquad\qquad \Longrightarrow \quad v = F_v^{-1}(u) = \Phi^{-1}\left(u \cdot \Phi(\bar{v})\right), \tag{12}$$

where $U(0,1)$ is the uniform distribution over the $[0,1]$ interval, and $\Phi^{-1}(\cdot)$ is the inverse normal *cdf*. Alternatively, rejection sampling could be used, or a combination of both approaches that reflects the (computationally) optimal acceptance probability for application of the rejection sampling approach; see, for example, Geweke (1991), Chopin (2011), and Botev (2017).[48]

To derive $\mu_{1:t-1,t+1:T}$, $\omega_{1:t-1,t+1:T}$, we now focus on the moments of the (unconstrained) missing-value problem stated in (9), understanding that draws for s_t are to be generated from the constrained shadow-rate problem in (8).

A.2 Shadow-rate VAR in companion form

Written in companion form, the VAR(p) in (4) is characterized by Markov dynamics of a state vector that tracks z_t and $p-1$ of its lags. Consequently, it is sufficient to consider no more than p lags and leads of z_t in the derivation of $\mu_{1:t-1,t+1:T}$, $\omega_{1:t-1,t+1:T}$.

We employ the following companion form notation for the VAR (omitting intercepts),

[48] However, in our application, potential gains from applying a combination approach appeared so far to be limited if not negative. At least in our MATLAB programming environment, direct application of the `trandn.m` routine provided by Botev (2017) underperformed relative to uniform-inverse-transform sampling. A likely cause for the somewhat surprising performance of the latter appears to be our use of large pre-generated random arrays as opposed to generating pseudo-random values one-at-a-time as done in the case of `trandn.m`.

adapted to the partitioning of z_t into x_t and s_t:

$$Z_t = \boldsymbol{A} Z_{t-1} + \boldsymbol{B}_t w_t \,, \qquad\qquad w_t \sim N(0, I) \,, \tag{13}$$

and let C_x and C_s be selection matrices so that $x_t = C_x Z_t$ and $s_t = C_s Z_t$.

To construct this companion form, consider for concreteness the case of a second-order system, with $p = 2$, and let

$$X_t = \begin{bmatrix} x_t \\ x_{t-1} \end{bmatrix} , \qquad S_t = \begin{bmatrix} s_t \\ s_{t-1} \end{bmatrix} , \qquad Z_t = \begin{bmatrix} X_t \\ S_t \end{bmatrix} = \begin{bmatrix} x_t \\ x_{t-1} \\ s_t \\ s_{t-1} \end{bmatrix} , \tag{14}$$

$$\text{with} \quad \boldsymbol{A} = \begin{bmatrix} A^1_{xx} & A^2_{xx} & A^1_{xs} & A^2_{xs} \\ I & 0 & 0 & 0 \\ A^1_{sx} & A^2_{sx} & A^1_{ss} & A^2_{ss} \\ 0 & 0 & I & 0 \end{bmatrix} , \qquad \boldsymbol{B}_t = \begin{bmatrix} B_{x,t} \\ 0 \\ B_{s,t} \\ 0 \end{bmatrix} , \tag{15}$$

where $B_{x,t}$ and $B_{s,t}$ are conformable partitions of a factorization $\Sigma_t^{0.5}$ of the variance-covariance matrix of VAR residuals in (4), so that $\Sigma_t = \Sigma_t^{0.5} \left(\Sigma_t^{0.5}\right)'$ and $\Sigma_t^{0.5} = \begin{bmatrix} B'_{x,t} & B'_{s,t} \end{bmatrix}'$.[49]

[49] Without loss of generality, we can, but do not have to, assume that $\Sigma_t^{0.5}$ is lower triangular. In our application, based on the VAR-SV model of Carriero, Clark, and Marcellino (2019), we have $\Sigma_t^{0.5} = A_0^{-1} \Lambda_t^{0.5}$, where A_0 is a unit-lower-triangular, and $\Lambda_t^{0.5}$ is a diagonal matrix of stochastic volatilities.

A.3 Moments of the missing-value problem

Given the VAR(p) structure of the model, and using the companion-form notation introduced above, the posterior density of the Gaussian missing-value problem in (9) simplifies as follows:

$$\begin{aligned} f\left(s_t \,\middle|\, s_{1:t-1}, s_{t+1:T}, \bar{\boldsymbol{Y}}\right) &= f\left(s_t \,\middle|\, s_{t-p:t-1}, s_{t+1:t+p}, x_{t-p:t+p}\right) \\ &= f\left(s_t \,\middle|\, Z_{t-1}, Z_{t+p}, x_t\right) \\ &= f\left(s_t \,\middle|\, Z_{t-1}, Z_{t+p} - Z_{t+p|t-1}, v_t^x\right), \end{aligned} \tag{16}$$

where $Z_{t+p|t-1} = E(Z_{t+p}|Z_{t-1}) = \boldsymbol{A}^{p+1} Z_{t-1}$ and $v_t^x = x_t - E(x_t|Z_{t-1}) = C_x v_t$.

Observations t with $t + p \leq T$: As stated above, we assume that we have observations for at least p initial lags of s_t at $t = 1$, and can thus always condition on $s_{t-p:t-1}$. Deferring a description of cases where $t + p > T$ for later, we first consider observations for t with $t + p \leq T$ and define the following signal vector:

$$\boldsymbol{\mathcal{Z}}_{t+p} = \begin{bmatrix} Z_{t+p} - Z_{t+p|t-1} \\ v_t^x \end{bmatrix} = \begin{bmatrix} \sum_{j=0}^{p} \boldsymbol{A}^{p-j} \boldsymbol{B}_{t+j} w_{t+j} \\ C_x \boldsymbol{B}_t w_t \end{bmatrix}. \tag{17}$$

The moments $\mu_{1:t-1,t+1:T}$ and $\omega_{1:t-1,t+1:T}$ follow from Gaussian signal extraction applied to the case of inference on s_t given the signal $\boldsymbol{\mathcal{Z}}_{t+p}$ and prior information captured by Z_{t-1}:

$$\mu_{1:t-1,t+1:T} = E(s_t|Z_{t-1}, Z_{t+1}, x_t) = E(s_t|Z_{t-1}) + \boldsymbol{J}_t \boldsymbol{\mathcal{Z}}_{t+p}, \tag{18}$$

$$\text{with} \quad \boldsymbol{J}_t = \text{Cov}\left(s_t, \boldsymbol{\mathcal{Z}}_{t+p} \,\middle|\, Z_{t-1}\right) \left(\text{Var}\left(\boldsymbol{\mathcal{Z}}_{t+p} \,\middle|\, Z_{t-1}\right)\right)^{-1}, \tag{19}$$

$$\text{Var}\left(\boldsymbol{\mathcal{Z}}_{t+p} \,\middle|\, Z_{t-1}\right) = \begin{bmatrix} \sum_{j=0}^{p} \boldsymbol{A}^{p-j} \boldsymbol{B}_{t+j} \boldsymbol{B}_{t+j}' \left(\boldsymbol{A}^{p-j}\right)' & \boldsymbol{A}^p \boldsymbol{B}_t \boldsymbol{B}_t' C_x' \\ C_x \boldsymbol{B}_t \boldsymbol{B}_t' \left(\boldsymbol{A}^p\right)' & C_x \boldsymbol{B}_t \boldsymbol{B}_t' C_x' \end{bmatrix}, \tag{20}$$

$$\text{Cov}\left(s_t, \boldsymbol{\mathcal{Z}}_{t+p} \,\middle|\, Z_{t-1}\right) = \begin{bmatrix} C_s \boldsymbol{B}_t \boldsymbol{B}_t' \left(\boldsymbol{A}^p\right)' \\ C_s \boldsymbol{B}_t \boldsymbol{B}_t' C_x' \end{bmatrix}, \tag{21}$$

$$\text{and} \quad \omega_{1:t-1,t+1:T} = \text{Var}\left(s_t | Z_{t-1}, Z_{t+1}, x_t\right) = C_s \boldsymbol{B}_t \boldsymbol{B}_t' C_s' - \text{Cov}\left(s_t, \boldsymbol{\mathcal{Z}}_{t+p} \,\middle|\, Z_{t-1}\right) \left(\text{Var}\left(\boldsymbol{\mathcal{Z}}_{t+p} \,\middle|\, Z_{t-1}\right)\right)^{-1} \text{Cov}\left(s_t, \boldsymbol{\mathcal{Z}}_{t+p} \,\middle|\, Z_{t-1}\right). \quad (22)$$

To compute the Kalman-smoothing gain $\boldsymbol{J}_t$ and residual variance $\text{Var}\left(s_t | Z_{t-1}, Z_{t+1}, x_t\right)$ efficiently, and robustly to numerical round-off errors (which could otherwise imply non-positive-definite values for variance-covariance matrices) we employ a QR factorization that builds on some of the fast-array algorithms presented by Kailath, Sayed, and Hassibi (2000).

Specifically, consider a factorization of the joint variance-covariance matrix of the signal, $\boldsymbol{\mathcal{Z}}_{t+p}$, and unknown state, s_t:[50]

$$\text{Var}_{t-1}\left(\begin{bmatrix} \boldsymbol{\mathcal{Z}}_{t+p} \\ s_t \end{bmatrix}\right) = \boldsymbol{L}\,\boldsymbol{L}' = \boldsymbol{M}\,\boldsymbol{M}', \quad (23)$$

where L and M are the following square matrices of length $N_z \cdot p + N_s$ along each dimension:

$$\boldsymbol{L} = \begin{bmatrix} \text{Var}_{t-1}\left(\boldsymbol{\mathcal{Z}}_{t+p}\right)^{0.5} & \boldsymbol{0} \\ \boldsymbol{J}_t \left(\text{Var}_{t-1}\left(\boldsymbol{\mathcal{Z}}_{t+p}\right)^{0.5}\right)' & \text{Var}_{t-1}\left(s_t | \boldsymbol{\mathcal{Z}}_{t+p}\right)^{0.5} \end{bmatrix} \quad (24)$$

$$\boldsymbol{M} = \begin{bmatrix} \boldsymbol{A}^p \boldsymbol{B}_t & \boldsymbol{A}^{p-1} \boldsymbol{B}_{t+1} & \dots & \boldsymbol{A}^1 \boldsymbol{B}_{t+p-1} & \boldsymbol{B}_{t+p} \\ C_x \boldsymbol{B}_t & 0 & \dots & \dots & 0 \\ C_s \boldsymbol{B}_t & 0 & \dots & \dots & 0 \end{bmatrix}. \quad (25)$$

The matrix $\boldsymbol{M}$ is straightforward to construct. Crucially, $\boldsymbol{L}$ is a lower triangular matrix, and its transpose, $\boldsymbol{L}'$, can directly be obtained from a QR factorization of $\boldsymbol{M}'$, $\boldsymbol{M}' = \boldsymbol{Q}\boldsymbol{L}'$ (where $\boldsymbol{Q}$ is an orthogonal matrix that can be ignored for our purpose). The Kalman-smoothing gain, $\boldsymbol{J}_t$, and the square root of the residual variance of s_t are contained in appropriate partitions of $\boldsymbol{L}$.

[50] For brevity, we let $\text{Var}_{t-1}(\cdot)$ denote $\text{Var}(\cdot | Z_{t-1})$. In addition, for any positive-(semi)definite square matrix $\boldsymbol{P}$, $\boldsymbol{P}^{0.5}$ denotes a (not necessarily positive-(semi)definite) lower-triangular factorization, such that $\boldsymbol{P} = \boldsymbol{P}^{0.5}\left(\boldsymbol{P}^{0.5}\right)'$.

Based on (16), it follows that $\text{Var}_{t-1}\left(s_t|\boldsymbol{\mathcal{Z}}_{t+p}\right) = \omega_{1:t-1,t+1:T}$, which is the desired second moment needed for the shadow-rate sampling problem in (8) of drawing s_t conditional on the remainder of the shadow-rate path.

Observations t with $t+p>T$: When the ELB is binding near the end of the data sample, in particular for t with $t+p>T$, the signal vector must be limited to include only leads of s_t and x_t up to T. Specifically, letting $t=T-k$ (with $k<p$), the adapted signal vector is shortened to a length of $N_z \cdot k + N_x$ as follows:

$$\boldsymbol{\mathcal{Z}}_{T,k} = \begin{bmatrix} Z_T - Z_{T|T-k-1} \\ v_t^x \end{bmatrix} = \begin{bmatrix} \sum_{j=0}^{k} \boldsymbol{H}_k \, \boldsymbol{A}^{k-j} \, \boldsymbol{B}_{t+j} \, w_{t+j} \\ C_x \, \boldsymbol{B}_t \, w_t \end{bmatrix}, \tag{26}$$

where $\boldsymbol{H}_k = \begin{bmatrix} I_{N_z \cdot k} & 0_{N_z \cdot (p-k)} \end{bmatrix}$ is a selection matrix selecting the first $N_z \cdot k$ elements out of a vector of length $N_z \cdot p$.[51] The expressions for $\boldsymbol{J}_t$ and $\text{Var}\left(s_t|Z_{t-1}, Z_{t+1}, x_t\right)$ in (19) and (22) are adjusted accordingly.

A.4 MCMC estimation of shadow-rate VAR

So far, this appendix has described a Gibbs sampler that generates draws for the shadow rate, according to (7), taking specific values for VAR parameters, $\{A_j\}_{j=1}^p$ and $\{\Sigma_t\}_{t=1}^T$, as given.[52] Here we describe how the shadow-rate Gibbs sampler is embedded into the MCMC estimation of the shadow-rate VAR system. (Our specification of the heteroskedasticity that is captured by $\{\Sigma_t\}_{t=1}^T$ follows Carriero, Clark, and Marcellino (2019), and details of generating draws from $\{A_j\}_{j=1}^p$ and $\{\Sigma_t\}_{t=1}^T$ follow their procedures.)[53]

[51] In the case of $t=T$ (and thus $k=0$), the signal vector collapses to $\boldsymbol{\mathcal{Z}}_{T,0} = v_t^x$.

[52] Given shadow-rate data, our implementation of the stochastic-volatility VAR (4) follows closely the setup of Carriero, Clark, and Marcellino (2019), where Σ_t can be broken further down into a set of slope parameters of a Cholesky factorization and a latent vector process representing stochastic volatilities. Nevertheless, for brevity, we refer here to $\{\Sigma_t\}_{t=1}^T$ as a set of VAR "parameters."

[53] Specifically, we let $v_t = A_0^{-1}\Lambda_t^{-0.5}\varepsilon_t$, where A_0 is a lower unit-triangular matrix, Λ_t is a diagonal matrix, and the vector of its diagonal elements is denoted λ_t, with $\log\lambda_t = \log\lambda_{t-1} + \eta_t$, $\eta_t \sim N(0,\Phi)$, and $\varepsilon_t \sim N(0,I)$. Other forms of heteroskedasticity could also be specified. For the purpose of our discussion, we

Denoting the mth MCMC draws of the VAR parameters $\{A_j\}_{j=1}^{p}$, $\{\Sigma_t\}_{t=1}^{T}$, and the shadow rates $\{s_t\}_{t=1}^{T}$, by $\boldsymbol{A}^m$, $\boldsymbol{\Sigma}^m$ and $\boldsymbol{S}^m$, respectively, and denoting (as before) the observed data by $\boldsymbol{Y}$, the MCMC sampler iterates over the following three blocks, for $m = 1, 2, \ldots, M$.

$$\boldsymbol{S}^{(m)} | \boldsymbol{A}^{(m-1)}, \boldsymbol{\Sigma}^{(m-1)}, \boldsymbol{Y} \tag{27}$$

$$\boldsymbol{A}^{(m)} | \boldsymbol{S}^{(m)}, \boldsymbol{\Sigma}^{(m-1)}, \boldsymbol{Y} \tag{28}$$

$$\boldsymbol{\Sigma}^{(m)} | \boldsymbol{S}^{(m)}, \boldsymbol{A}^{(m)}, \boldsymbol{Y} \tag{29}$$

Henceforth, we will refer to iterations over (27)– (29), as "the MCMC sampler." We use $M = 1200$ draws, of which an initial 200 burn-in draws are discarded.

The first block of the MCMC sampler, given by (27), consists of a sequence of Gibbs sampling steps, iterating over (8) for $t = 1, 2, \ldots, T$, with details described earlier in this appendix. The Gibbs sampler for the truncated MVN is a single-move sampler that draws one observation of s_t at a time (conditional on previously sampled values for all others). Consequently, a single pass from the Gibbs sampler for the truncated normal does not generate a direct draw from $\boldsymbol{S}^{(m)} | \boldsymbol{A}^{(m-1)}, \boldsymbol{\Sigma}^{(m-1)}, \boldsymbol{Y}$.[54] Nevertheless, repeated iterations over (27), (28), and (29), with each pass over the shadow-rate block in (27) captured by a single pass of the Gibbs sampler in (10), will eventually generate draws from the joint posterior density of $\boldsymbol{A}$, $\boldsymbol{\Sigma}$, and $\boldsymbol{S}$.[55]

In order to achieve higher computational efficiency, we conduct multiple passes of the Gibbs sampler at every iteration, m, of the MCMC sampler.[56] In doing so, we exploit

subsume the slope parameters A_0 and variance parameters Ω in the block of parameters denoted by $\{\Sigma_t\}_{t=1}^{T}$. Our MCMC sampler also reflects the ordering of steps in SV estimation recommended by Del Negro and Primiceri (2015).

[54] In contrast, in the case of the linear missing-value problem in (6), multi-move sampling is feasible. The missing-value problem has a linear Gaussian state space representation, and a Kalman-smoothing sampler can directly draw from the (untruncated) multivariate normal distribution of the problem, for example, by employing the methods described in Durbin and Koopman (2002).

[55] Formally, the mth draw from the shadow-rate block in (27) is then obtained by a single iteration over $s_t^{(m)} \mid s_{1:t-1}^{(m)}, s_{t+1:T}^{(m-1)}, \boldsymbol{A}^{(m-1)}, \boldsymbol{\Sigma}^{(m-1)}, \boldsymbol{Y}$ for $T = 1, 2, \ldots, T$ and holding m fixed.

[56] Our approach of embedding the procedures for drawing from the truncated MVN into the MCMC sampler with multiples passes at each MCMC step builds on ideas developed by Waggoner and Zha (1999) in the context of simulating forecasts under soft restrictions.

the fact that the Kalman-smoothing gains, $\boldsymbol{J}_t$, and residual variances $\text{Var}\left(s_t|Z_{t-1}, Z_{t+1}, x_t\right)$, described in (19) and (22) above, depend only on prior draws of the VAR parameters $\boldsymbol{A}^{(m-1)}$ and $\boldsymbol{\Sigma}^{(m-1)}$, but not the sampled path for the shadow rate, $\boldsymbol{S}^{(m)}$. As noted already by Geweke (1991), the second-moment matrices required for multiple passes of the Gibbs sampler for the truncated MVN need to be computed only once (given $\boldsymbol{A}^{(m-1)}$ and $\boldsymbol{\Sigma}^{(m-1)}$), which makes it computationally relatively cheap to conduct multiple Gibbs passes. Denoting the number of Gibbs passes by N, we retain only the output sampled in the Nth pass, treating the initial $N-1$ as burn-in passes. Similar to Waggoner and Zha (1999), the motivation behind our approach is to hand over a draw $\boldsymbol{S}^{(m)}$ to the remaining MCMC steps that avoids the higher serial dependence between MCMC steps resulting from the previously described single-pass approach, while also being computationally relatively cheap to produce compared to other elements of the MCMC setup.

Formally, for every MCMC draw m, we implement the shadow-rate sampling block in (27) with N Gibbs passes as follows: For each $n = 1, 2, \ldots, N$, (and holding m fixed) iterate over

$$s_t^{(m,n)} \,\Big|\, s_{1:t-1}^{(m,n)}, s_{t+1:T}^{(m,n-1)}, \boldsymbol{Y} \qquad\qquad \text{for } t = 1, 2, \ldots, T\,. \tag{30}$$

For each m, we initialize the first Gibbs pass with $s_t^{(m,0)} = s_t^{(m-1,N)}$, $\forall\, t$, and we retain $\boldsymbol{S}^{(m)} = \{s_t^{(m,N)}\}_{t=1}^{T}$ as the mth draw of the sequence of shadow rates. In our application, we employ $N = 201$ Gibbs passes over (30), and thus 200 burn-in passes for every step, m, of the MCMC sampler.

References

[1] Aruoba, S. Boragan, Marko Mlikota, Frank Schorfheide, and Sergio Villalvazo (2021), "SVARs with occasionally-binding constraints," Working Paper 28571, National Bureau of Economic Research, https://doi.org/10.3386/w28571.

[2] Bauer, Michael D., and Glenn D. Rudebusch (2016), "Monetary policy expectations at the zero lower bound," *Journal of Money, Credit and Banking*, 48, 1439–1465, https://doi.org/10.1111/jmcb.12338.

[3] Bäurle, Gregor, Daniel Kaufmann, Sylvia Kaufmann, and Rodney W. Strachan (2016), "Changing dynamics at the zero lower bound," Working Paper 2016-16, Swiss National Bank, https://ideas.repec.org/p/snb/snbwpa/2016-16.html.

[4] Berg, Tim Oliver (2017), "Forecast accuracy of a BVAR under alternative specifications of the zero lower bound," *Studies in Nonlinear Dynamics & Econometrics*, 21, 1–29, https://doi.org/10.1515/snde-2015-0084.

[5] Bernanke, Ben S., and Alan S. Blinder (1992), "The federal funds rate and the channels of monetary transmission," *The American Economic Review*, 82, 901–21, http://ideas.repec.org/a/aea/aecrev/v82y1992i4p901-21.html.

[6] Billi, Roberto M. (2020), "Output gaps and robust monetary policy rules," *International Journal of Central Banking*, 16, 125–152, https://ideas.repec.org/a/ijc/ijcjou/y2020q1a4.html.

[7] Black, Fischer (1995), "Interest rates as options," *The Journal of Finance*, 50, 1371–1376, https://doi.org/10.1111/j.1540-6261.1995.tb05182.x.

[8] Board of Governors of the Federal Reserve System (2020), "Monetary Policy Report," February, https://www.federalreserve.gov/monetarypolicy/2020-02-mpr-summary.htm.

[9] Botev, Z. I. (2017), "The normal law under linear restrictions: simulation and estimation via minimax tilting," *Journal of the Royal Statistical Society: Series B (Statistical Methodology)*, 79, 125–148, https://doi.org/10.1111/rssb.12162.

[10] Canova, Fabio (2007), *Methods for Applied Macroeconomic Research*: Princeton University Press, https://muse.jhu.edu/book/64846.

[11] Carriero, Andrea, Todd E. Clark, and Massimiliano Marcellino (2019), "Large Bayesian vector autoregressions with stochastic volatility and non-conjugate priors," *Journal of Econometrics*, 212, 137–154, https://doi.org/10.1016/j.jeconom.2019.04.024.

[12] Carriero, Andrea, Todd E. Clark, Massimiliano Marcellino, and Elmar Mertens (2021), "Addressing COVID-19 outliers in BVARs with stochastic volatility," Working Paper 2021-02, Federal Reserve Bank of Cleveland, https://doi.org/10.26509/frbc-wp-202102.

[13] Chan, Joshua C.C., and Eric Eisenstat (2018), "Bayesian model comparison for time-varying parameter VARs with stochastic volatility," *Journal of Applied Econometrics*, 33, 509–532, https://doi.org/10.1002/jae.2617.

[14] Chan, Joshua C.C., and Ivan Jeliazkov (2009), "Efficient simulation and integrated likelihood estimation in state space models," *International Journal of Mathematical Modelling and Numerical Optimization*, 1, 101–120, https://doi.org/10.1504/IJMMNO.2009.030090.

[15] Chan, Joshua C.C., and Rodney Strachan (2014), "The Zero Lower Bound: Implications for Modelling the Interest Rate," Working Paper series 42-14, Rimini Centre for Economic Analysis, https://ideas.repec.org/p/rim/rimwps/42_14.html.

[16] Chopin, Nicolas (2011), "Fast simulation of truncated Gaussian distributions," *Chopin, Nicolas*, 21, 275–288, https://doi.org/10.1007/s11222-009-9168-1.

[17] Christensen, Jens H.E., and Glenn D. Rudebusch (2015), "Estimating shadow-rate term structure models with near-zero yields," *Journal of Financial Econometrics*, 13, 226–259, https://doi.org/10.1093/jjfinec/nbu010.

[18] Christiano, Lawrence J., Martin Eichenbaum, and Charles Evans (1996), "The effects of monetary policy shocks: Evidence from the flow of funds," *The Review of Economics and Statistics*, 78, 16–34, https://doi.org/10.2307/2109845.

[19] Christiano, Lawrence J., Martin Eichenbaum, and Charles L. Evans (1999), "Monetary policy shocks: What have we learned and to what end?" in *Handbook of Macroeconomics* eds. by John B. Taylor, and Michael Woodford, Amsterdam: Elsevier, chap. 2, https://ideas.repec.org/h/eee/macchp/1-02.html, Volume 1A.

[20] Clark, Todd E. (2011), "Real-time density forecasts from Bayesian vector autoregressions with stochastic volatility," *Journal of Business and Economic Statistics*, 29, 327–341, https://doi.org/10.1198/jbes.2010.09248.

[21] Clark, Todd E., and Francesco Ravazzolo (2015), "Macroeconomic forecasting performance under alternative specifications of time-varying volatility," *Journal of Applied Econometrics*, 30, 551–575, https://doi.org/10.1002/jae.2379.

[22] Cogley, Timothy, Giorgio E. Primiceri, and Thomas J. Sargent (2010), "Inflation-gap persistence in the US," *American Economic Journal: Macroeconomics*, 2, 43–69, https://doi.org/10.1257/mac.2.1.43.

[23] Cogley, Timothy, and Thomas J. Sargent (2005), "Drift and volatilities: Monetary policies and outcomes in the post WWII US," *Review of Economic Dynamics*, 8, 262–302, https://doi.org/10.1016/j.red.2004.10.009.

[24] Cong, Yulai, Bo Chen, and Mingyuan Zhou (2017), "Fast simulation of hyperplane-truncated multivariate normal distributions," *Bayesian Analysis*, 12, 1017–1037, https://doi.org/10.1214/17-BA1052.

[25] D'Agostino, Antonello, Luca Gambetti, and Domenico Giannone (2013), "Macroeconomic forecasting and structural change," *Journal of Applied Econometrics*, 28, 82–101, https://doi.org/10.1002/jae.1257.

[26] Damien, Paul, and Stephen G. Walker (2001), "Sampling truncated normal, beta, and gamma densities," *Journal of Computational and Graphical Statistics*, 10, 206–215, https://doi.org/10.1198/10618600152627906.

[27] Debortoli, Davide, Jordi Gali, and Luca Gambetti (2019), "On the empirical (ir)relevance of the zero lower bound constraint," in *NBER Macroeconomics Annual 2019, Volume 34*: National Bureau of Economic Research, Inc, https://doi.org/10.1086/707177.

[28] Del Negro, Marco, Domenico Giannone, Marc P. Giannoni, and Andrea Tambalotti (2017), "Safety, liquidity, and the natural rate of interest," *Brookings Papers on Economic Activity*, 48, 235–316, https://doi.org/10.1353/eca.2017.0003.

[29] Del Negro, Marco, and Giorgio E. Primiceri (2015), "Time varying structural vector autoregressions and monetary policy: A corrigendum," *Review of Economic Studies*, 82, 1342–1345, https://doi.org/10.1093/restud/rdv024.

[30] Diebold, Francis X., and Roberto S. Mariano (1995), "Comparing predictive accuracy," *Journal of Business and Economic Statistics*, 13, 253–63, https://doi.org/10.2307/1392185.

[31] Durbin, J., and S.J. Koopman (2002), "A simple and efficient simulation smoother for state space time series analysis," *Biometrika*, 89, 603–615, https://doi.org/10.1093/biomet/89.3.603.

[32] Gelfand, Alan E., Adrian F. M. Smith, and Tai-Ming Lee (1992), "Bayesian analysis of constrained parameter and truncated data problems using Gibbs sampling," *Journal of the American Statistical Association*, 87, 523–532, https://doi.org/10.2307/2290286.

[33] Geweke, John (1991), "Efficient simulation from the multivariate normal and student-t distributions subject to linear constraints and the evaluation of constraint probabilities," in *Computing Science and Statistics: Proceedings of the Twenty-Third Symposium on the Interface* ed. by E. M. Keramidas, 571–578, Fairfax: Interface Foundation of North America, Inc. https://citeseerx.ist.psu.edu/viewdoc/download?doi=10.1.1.26.6892&rep=rep1&type=pdf.

[34] Gonzalez-Astudillo, Manuel, and Jean-Philippe Laforte (2020), "Estimates of r* consistent with a supply-side structure and a monetary policy rule for the U.S. economy," Finance and Economics Discussion Series 2020-085, Board of Governors of the Federal Reserve System, https://doi.org/10.17016/FEDS.2020.085.

[35] Gust, Christopher, Edward Herbst, David López-Salido, and Matthew E. Smith (2017), "The empirical implications of the interest-rate lower bound," *American Economic Review*, 107, 1971–2006, https://doi.org/10.1257/aer.20121437.

[36] Horrace, William C. (2005), "Some results on the multivariate truncated normal distribution," *Journal of Multivariate Analysis*, 94, 209–221, https://doi.org/10.1016/j.jmva.2004.10.007.

[37] Iwata, Shigeru, and Shu Wu (2006), "Estimating monetary policy effects when interest rates are close to zero," *Journal of Monetary Economics*, 53, 1395–1408, https://doi.org/10.1016/j.jmoneco.2005.05.009.

[38] Johannsen, Benjamin K., and Elmar Mertens (2021), "A time series model of interest rates with the effective lower bound," *Journal of Money, Credit and Banking*, https://doi.org/10.1111/jmcb.12771.

[39] Joslin, Scott, Anh Le, and Kenneth J. Singleton (2013), "Why Gaussian macro-finance term structure models are (nearly) unconstrained factor-VARs," *Journal of Financial Economics*, 109, 604–622, https://doi.org/10.1016/j.jfineco.2013.04.

[40] Kailath, Thomas, Ali H. Sayed, and Babak Hassibi (2000), *Linear Estimation*, Prentice Hall Information and System Sciences Series: Pearson Publishing, http://infoscience.epfl.ch/record/233814.

[41] Kim, Don, and Kenneth J. Singleton (2012), "Term structure models and the zero bound: An empirical investigation of Japanese yields," *Journal of Econometrics*, 170, 32–49, https://doi.org/10.1016/j.jeconom.2011.12.005.

[42] Koop, Gary (2003), *Bayesian Econometrics*: Wiley-Interscience, https://pureportal.strath.ac.uk/en/publications/bayesian-econometrics.

[43] Krippner, Leo (2013), "Measuring the stance of monetary policy in zero lower bound environments," *Economics Letters*, 118, 135–138, https://doi.org/10.1016/j.econlet.2012.10.011.

[44] ——— (2015), *Zero Lower Bound Term Structure Modeling: A Practitioner's Guide*: Palgrave Macmillan, https://doi.org/10.1057/9781137401823.

[45] ——— (2020), "A note of caution on shadow rate estimates," *Journal of Money, Credit and Banking*, 52, 951–962, https://doi.org/10.1111/jmcb.12613.

[46] Lombardi, Marco J., and Feng Zhu (2018), "A shadow policy rate to calibrate U.S. monetary policy at the zero lower bound," *International Journal of Central Banking*, 14, 305–346, https://ideas.repec.org/a/ijc/ijcjou/y2018q4a8.html.

[47] Mavroeidis, Sophocles (2020), "Identification at the zero lower bound," October, *mimeo*, University of Oxford.

[48] Nakajima, Jouchi (2011), "Monetary policy transmission under zero interest rates: An extended time-varying parameter vector autoregression approach," IMES Discussion Paper Series 2011-E-8, Bank of Japan, https://www.imes.boj.or.jp/research/abstracts/english/11-E-08.html.

[49] Primiceri, Giorgio E. (2005), "Time varying structural vector autoregressions and monetary policy," *Review of Economic Studies*, 72, 821–852, https://doi.org/10.1111/j.1467-937X.2005.00353.x.

[50] Reifschneider, David, and John C. Williams (2000), "Three lessons for monetary policy in a low-inflation era," *Journal of Money, Credit and Banking*, 32, 936–966, https://doi.org/10.2307/2601151.

[51] Robert, Christian P. (1995), "Simulation of truncated normal variables," *Statistics and Computing*, 5, 121–125, https://doi.org/10.1007/BF00143942.

[52] Rotemberg, Julio J., and Michael Woodford (1997), "An optimization-based econometric framework for the evaluation of monetary policy," in *NBER Macroeconomics Annual 1997* eds. by Ben S. Bernanke, and Julio J. Rotemberg, Cambridge (MA): The MIT Press, 297–346, https://doi.org/10.1086/654340.

[53] Schorfheide, Frank, and Dongho Song (2020), "Real-time forecasting with a (standard) mixed-frequency VAR during a pandemic," Working Paper 20-26, Federal Reserve Bank of Philadelphia, https://doi.org/10.21799/frbp.wp.2020.26.

[54] Swanson, Eric T., and John C. Williams (2014), "Measuring the Effect of the Zero Lower Bound on Medium- and Longer-Term Interest Rates," *American Economic Review*, 104, 3154–3185, https://doi.org/10.1257/aer.104.10.3154.

[55] Taylor, John B. (1993), "Discretion versus policy rules in practice," *Carnegie-Rochester Conference Series on Public Policy*, 39, 195–214, https://doi.org/10.1016/0167-2231(93)90009-L.

[56] ——— (1999), *Monetary Policy Rules*: University of Chicago Press, http://www.nber.org/books/tayl99-1.

[57] Waggoner, Daniel F., and Tao Zha (1999), "Conditional forecasts in dynamic multivariate models," *The Review of Economics and Statistics*, 81, 639–651, https://doi.org/10.1162/003465399558508.

[58] West, Kenneth D. (1996), "Asymptotic inference about predictive ability," *Econometrica*, 64, 1067–1084, https://doi.org/10.2307/2171956.

[59] Wu, Jing Cynthia, and Fan Dora Xia (2016), "Measuring the macroeconomic impact of monetary policy at the zero lower bound," *Journal of Money, Credit and Banking*, 48, 253–291, https://doi.org/10.1111/jmcb.12300.

[60] ——— (2020), "Negative interest rate policy and the yield curve," *Journal of Applied Econometrics*, 35, 653–672, https://doi.org/10.1002/jae.2767.

[61] Wu, Jing Cynthia, and Ji Zhang (2019), "A shadow rate New Keynesian model," *Journal of Economic Dynamics and Control*, 107, p. 103728, https://doi.org/10.1016/j.jedc.2019.103728.

Table 1: List of variables

Variable	FRED-MD code	transformation	Minnesota prior
Real Income	RPI	$\Delta \log(x_t) \cdot 1200$	0
Real Consumption	DPCERA3M086SBEA	$\Delta \log(x_t) \cdot 1200$	0
IP	INDPRO	$\Delta \log(x_t) \cdot 1200$	0
Capacity Utilization	CUMFNS		1
Unemployment	UNRATE		1
Nonfarm Payrolls	PAYEMS	$\Delta \log(x_t) \cdot 1200$	0
Hours	CES0600000007		0
Hourly Earnings	CES0600000008	$\Delta \log(x_t) \cdot 1200$	0
PPI (Fin. Goods)	WPSFD49207	$\Delta \log(x_t) \cdot 1200$	1
PPI (Metals)	PPICMM	$\Delta \log(x_t) \cdot 1200$	1
PCE Prices	PCEPI	$\Delta \log(x_t) \cdot 1200$	1
Federal Funds Rate	FEDFUNDS		1
Housing Starts	HOUST	$\log(x_t)$	1
S&P 500	SP500	$\Delta \log(x_t) \cdot 1200$	0
USD / GBP FX Rate	EXUSUKx	$\Delta \log(x_t) \cdot 1200$	0
5-Year Yield	GS5		1
10-Year Yield	GS10		1
Baa Spread	BAAFFM		1

Note: Data obtained from the 2020:10 vintage of FRED-MD. Monthly observations from 1959:03 to 2020:09. Entries in the column "Minnesota prior" report the prior mean on the first own-lag coefficient of the corresponding variable in each BVAR. Prior means on all other VAR coefficients are set to zero.

Table 2: Relative RMSE of mean forecasts

					Relative to Standard ...							
	Standard				Truncated				Shadow rate			
Variable / Horizon	3	6	12	24	3	6	12	24	3	6	12	24
Real Income	15.68	15.57	15.86	16.83	1.00	1.00*	1.00	1.00	1.00	1.00	1.00	0.99
Real Consumption	18.58	18.81	19.13	20.13	1.00	1.00	1.00	1.00	1.00	1.00	1.00	1.00
IP	18.95	17.51	17.99	19.08	0.99	1.01	1.01	0.99*	1.00	1.00	1.01	1.01
Capacity Utilization	2.78	2.22	2.58	3.66	1.00	1.03	1.16	1.30	1.01	1.01	1.08	1.30***
Unemployment	1.56	1.65	1.68	1.90	1.00	1.00	1.01**	1.11**	1.00	1.00	0.99	1.00
Nonfarm Payrolls	16.62	16.03	16.42	17.24	1.00	1.00*	1.00	1.00	1.00	1.00	1.00	1.00
Hours	0.45	0.37	0.40	0.48	1.01	1.02*	1.13	1.35	1.06	1.01	1.00	1.08
Hourly Earnings	2.45	2.35	2.45	2.81	1.00	0.99	0.97	0.92**	0.99	1.01	1.00	0.96***
PPI (Fin. Goods)	8.54	8.30	8.49	8.82	1.00	0.99	0.97	0.94	1.02	1.03	1.03	0.99
PPI (Metals)	38.34	37.54	35.43	29.93	1.01	1.00	0.99	1.01	1.01	1.01	1.01	0.99**
PCE Prices	2.40	2.30	2.65	3.23	0.98*	0.95	0.90	0.77	1.06**	1.07*	1.09	1.06
Federal Funds Rate	0.59	0.92	1.50	1.82	0.46*	0.48	0.58	1.02	0.36*	0.36	0.34	0.52**
Housing Starts	0.11	0.13	0.20	0.35	1.03	1.00	1.00	1.08	1.05	1.06	1.04	0.95
S&P 500	45.71	42.47	42.20	41.46	1.01	1.02	1.03	1.04	0.98*	0.99	0.99	0.99
USD / GBP FX Rate	26.20	24.13	24.07	23.93	1.01	1.00	1.00	1.01	0.99	0.99*	0.99	0.97***
5-Year Yield	0.52	0.76	1.04	1.32	1.01	1.05	1.29	1.93	0.93	0.92	0.77**	0.70**
10-Year Yield	0.48	0.73	1.00	1.14	1.05	1.06**	1.34	2.27	0.98	0.95	0.81	0.64**
Baa Spread	0.87	1.27	1.71	1.40	0.96	1.04	1.25	2.26	1.00	0.97	0.89	0.83

Note: Comparison of "Standard" (baseline, in denominator of relative comparisons) against "Truncated" and "Shadow rate." Values below 1 indicate improvement over baseline. Evaluation window from 2009:01 through 2020:09. Significance assessed by Diebold-Mariano-West test using Newey-West standard errors with $h+1$ lags. Due to the close behavior of some of the models compared, and rounding of the reported values, a few comparisons show a significant relative RMSE of 1.00. These cases arise from persistent differences in performance that are, however, too small to be relevant after rounding.

Table 3: Relative MAE of median forecasts

					Relative to Standard ...							
	Standard				Truncated				Shadow rate			
Variable / Horizon	3	6	12	24	3	6	12	24	3	6	12	24
Real Income	5.82	5.56	5.65	6.00	1.01**	1.02	1.04	0.99	1.00	1.00	1.00	1.00
Real Consumption	5.32	5.40	5.44	6.18	1.01	1.01	1.01	0.96	1.01	1.00	1.03	1.01
IP	7.57	7.18	7.38	8.03	0.99*	1.02	1.02	0.95	1.02*	1.01	1.06**	1.11**
Capacity Utilization	0.99	1.28	1.82	2.82	1.00	1.04	1.15	1.19	1.04***	1.08**	1.17**	1.43***
Unemployment	0.46	0.54	0.69	1.10	1.00	1.00	1.09***	1.28***	1.01**	1.02	1.03	1.04
Nonfarm Payrolls	3.38	3.13	3.25	3.68	1.00	1.02*	1.06**	1.14***	1.01	1.01	1.05**	1.11**
Hours	0.22	0.23	0.26	0.32	1.00	1.03*	1.13	1.40*	1.04*	1.03	1.05	1.19**
Hourly Earnings	1.82	1.76	1.86	2.23	1.00	0.99	0.94	0.88**	1.00	1.02	1.01	0.97*
PPI (Fin. Goods)	6.40	6.20	6.33	6.67	1.00	0.99	0.97	0.93	1.02	1.01	1.01	0.99
PPI (Metals)	28.13	27.83	26.60	23.08	1.01	1.00	0.99	1.01	1.01	1.00	1.00	0.99
PCE Prices	1.78	1.76	2.10	2.65	0.98**	0.96*	0.88*	0.76*	1.04	1.06	1.07	1.05
Federal Funds Rate	0.29	0.52	0.93	1.39	0.48**	0.59	0.69	0.77	0.26***	0.30**	0.30**	0.35***
Housing Starts	0.08	0.10	0.15	0.24	1.03	0.98	0.97	1.12	1.03	1.01	0.94	0.84
S&P 500	31.48	29.16	28.91	26.95	1.01	1.03	1.03	1.05	0.97**	0.98**	0.98	0.99
USD / GBP FX Rate	19.64	18.33	18.38	18.13	1.01**	1.01	1.01	1.04	0.99	0.99*	0.98	0.97**
5-Year Yield	0.39	0.61	0.86	1.06	0.99	1.03	1.26	1.56	0.89	0.95	0.81	0.73*
10-Year Yield	0.37	0.59	0.84	0.91	1.02*	1.06**	1.29	1.82	0.95	0.98	0.83	0.78
Baa Spread	0.52	0.76	1.08	1.05	0.98	1.00	1.03	1.25	1.01	1.03	0.96	0.92

Note: Comparison of "Standard" (baseline, in denominator of relative comparisons) against "Truncated" and "Shadow rate." Values below 1 indicate improvement over baseline. Evaluation window from 2009:01 through 2020:09. Significance assessed by Diebold-Mariano-West test using Newey-West standard errors with $h + 1$ lags.

Table 4: Relative CRPS of density forecasts

					Relative to Standard ...							
	Standard				Truncated				Shadow rate			
Variable / Horizon	3	6	12	24	3	6	12	24	3	6	12	24
Real Income	5.08	4.93	5.12	5.88	1.00	1.01	1.01	1.01	0.99	0.99	1.00	1.01
Real Consumption	5.07	4.91	5.01	5.78	1.00	1.00	1.00	1.00	1.00	1.00	1.02**	1.02
IP	6.02	5.87	6.18	6.99	1.00	1.01	1.01	0.99	1.01**	1.01	1.04**	1.07**
Capacity Utilization	0.78	1.00	1.44	2.32	1.01	1.03	1.10	1.15**	1.04***	1.05*	1.12***	1.24***
Unemployment	0.37	0.47	0.59	0.86	1.00	1.00	1.05***	1.18***	1.01*	1.01	1.02	1.03
Nonfarm Payrolls	2.94	2.79	2.99	3.43	1.00	1.01**	1.03*	1.07***	1.00	1.01	1.02**	1.05***
Hours	0.17	0.18	0.21	0.28	1.00	1.02**	1.11*	1.22**	1.04**	1.04*	1.05	1.13**
Hourly Earnings	1.37	1.34	1.45	1.84	1.00	1.00	0.99	0.97***	1.00	1.01	1.00	1.00
PPI (Fin. Goods)	4.78	4.63	4.72	5.22	1.00	1.00	0.99	0.98	1.01	1.01	1.02	1.00
PPI (Metals)	20.63	20.31	20.37	20.63	1.00	1.00	1.00	1.01	1.00	1.00	1.00	1.01*
PCE Prices	1.31	1.32	1.50	1.94	0.99**	0.97*	0.95	0.90*	1.04	1.04	1.06	1.04
Federal Funds Rate	0.21	0.38	0.68	1.05	0.47**	0.55	0.62	0.70	0.28***	0.30**	0.29**	0.34***
Housing Starts	0.06	0.07	0.11	0.19	1.01	1.01	1.02	1.12	1.02	1.00	0.96	0.90
S&P 500	24.00	22.40	22.86	24.77	1.01*	1.01	1.02	1.02	0.99	0.99*	1.00	1.02***
USD / GBP FX Rate	14.68	13.90	14.14	15.49	1.01	1.00	1.00	1.02	0.99	0.99	0.99	1.00
5-Year Yield	0.28	0.44	0.62	0.81	0.99	1.04	1.20	1.40	0.92	0.93	0.81**	0.69***
10-Year Yield	0.27	0.42	0.59	0.70	1.01	1.06**	1.24*	1.60	0.96	0.95	0.86	0.80**
Baa Spread	0.37	0.54	0.74	0.87	0.99	1.00	1.06	1.21	1.01	1.01	0.96	1.00

Note: Comparison of "Standard" (baseline, in denominator of relative comparisons) against "Truncated" and "Shadow rate." Values below 1 indicate improvement over baseline. Evaluation window from 2009:01 through 2020:09. Significance assessed by Diebold-Mariano-West test using Newey-West standard errors with $h + 1$ lags.

Table 5: Comparison against plug-in VAR with Krippner shadow rates

	RMSE				MAE				CRPS			
Variable / Horizon	3	6	12	24	3	6	12	24	3	6	12	24
Real Income	1.00	1.00*	1.00	0.98***	0.99	0.99	1.00	0.99	0.99**	0.99	0.99*	0.99
Real Consumption	1.00	1.00	1.00	1.00	0.99	0.98*	0.98	0.96**	1.00	0.99**	0.98*	0.98*
IP	1.01	1.00	1.01	0.99	1.02	1.02	1.04	0.97	1.01	1.01	1.01	0.98
Capacity Utilization	0.99	1.03*	1.07	1.12	1.02	1.05	1.09	1.13	1.00	1.03	1.05	1.06
Unemployment	1.00	1.00	1.00	1.06	0.99	0.95*	0.90*	1.06	0.98	0.96*	0.95*	1.01
Nonfarm Payrolls	1.00	1.00	1.00	1.00	0.99	0.99	0.98	0.99	1.00	0.99	0.98***	0.98
Hours	1.01	0.98	0.97	1.04	0.98	0.97	0.97	1.02	0.99	0.97	0.98	1.05
Hourly Earnings	1.00	1.00	1.01	0.96*	0.99	1.01	0.99	0.97	0.99	1.01	1.01	1.01
PPI (Fin. Goods)	0.99	0.98	0.97**	0.97	0.98	0.98	0.97	0.97	0.98	0.98*	0.97*	0.98
PPI (Metals)	0.99	0.99*	0.99	0.99	0.99	0.99	0.99	0.98	0.99	0.99**	0.99	1.00
PCE Prices	1.00	0.96*	0.95*	0.92*	0.99	0.96**	0.96	0.94	0.98	0.96**	0.95	0.95
Policy Rate	0.83*	0.88*	0.89	1.02	0.83	0.83	0.85	0.97	0.84	0.85	0.89	0.99
Housing Starts	1.01	1.04	1.08	1.01	0.97	1.00	0.95	0.86	0.98	0.99	0.96	0.90
S&P 500	1.00	1.00	1.00	0.99	0.96*	0.98	0.99	0.96***	0.98	0.99	0.99	0.99
USD / GBP FX Rate	1.01	1.01	1.00	0.99	1.03*	1.01	1.02	0.99	1.01	1.00	1.00	0.99
5-Year Yield	1.04	1.09*	1.05	0.98	1.02	1.05	0.96	0.81**	1.00	1.02	0.97	0.86**
10-Year Yield	0.98	1.00	0.93	0.80**	0.96	0.98	0.89	0.69**	0.97	0.97	0.90	0.78***
Baa Spread	1.02	1.09	0.97	0.74**	0.93	0.90	0.85	0.72**	0.95	0.94	0.84	0.80***

Note: Comparison of "Krippner (plug-in VAR)" (baseline, in denominator) against "Shadow-rate VAR." Values below 1 indicate improvement over baseline. Evaluation window from 2009:01 through 2020:09. Significance assessed by Diebold-Mariano-West test using Newey-West standard errors with $h+1$ lags. Due to the close behavior of some of the models compared, and rounding of the reported values, one of the comparisons shows a significant ratio of 1.00. This case arises from persistent differences in performance that are, however, too small to be relevant after rounding.

Table 6: Comparison against plug-in VAR with Wu-Xia shadow rates

	RMSE				MAE				CRPS			
Variable / Horizon	3	6	12	24	3	6	12	24	3	6	12	24
Real Income	1.00	1.00**	1.00	0.98***	1.00	0.98*	0.98	0.99	1.00	0.99*	0.99	1.00
Real Consumption	1.00	1.00	1.00	1.00	0.98	0.98	1.00	0.99	1.00	1.00	1.00	1.00
IP	1.00	1.00	1.00	1.00	1.01	1.01	1.02	1.00	1.01	1.01	1.01	1.01
Capacity Utilization	0.97	1.00	1.00	1.03	0.98	0.98	1.00	1.07	0.98	0.99	0.99	1.01
Unemployment	1.00	1.00	1.00	1.04	0.99	0.95***	0.93**	1.06	0.99**	0.97**	0.96**	1.00
Nonfarm Payrolls	1.00	1.00	1.00	1.00	0.98**	0.98*	0.99	1.05	0.99**	0.98**	0.99	1.01
Hours	0.98*	0.97**	0.95	1.02	0.96***	0.93**	0.93	1.01	0.98*	0.95**	0.96	1.05
Hourly Earnings	0.99	0.99	0.99	0.97	0.99	1.01	0.99	0.97	0.99	1.00	0.99	1.01
PPI (Fin. Goods)	1.02	1.01	1.01	0.98	1.01	1.02	1.02*	0.98	1.01	1.01	1.01	0.99
PPI (Metals)	1.00	1.00	1.00	0.99	1.00	0.99	1.00	0.99	1.00	1.00	1.00	1.01*
PCE Prices	1.02	1.00	1.01	0.99	1.02	1.00	1.00	0.99	1.00	0.99	1.00	0.99
Policy Rate	0.80**	0.89**	0.95	1.10**	0.76**	0.82**	0.85*	0.97	0.77**	0.86**	0.94	1.00
Housing Starts	1.02	1.05	1.11	1.13	0.99	1.01	0.98	0.94	0.99	0.99	1.00	1.00
S&P 500	1.01	1.00	0.99	0.99	0.98	0.98**	0.99	0.99	1.00	0.99	0.99	1.01*
USD / GBP FX Rate	0.99	1.00	1.00	0.98	1.01	1.00	1.00	0.99	0.99	1.00	1.00	1.00
5-Year Yield	1.04	1.05	1.02	0.98	1.00	1.00	0.91	0.83	1.02	1.01	0.96	0.90
10-Year Yield	1.01	1.02	0.95	0.79**	0.99	1.01	0.96	0.77*	1.00	1.01	0.94	0.83**
Baa Spread	1.02	1.18	1.07	0.85	1.02	1.02	0.95	0.86	1.02	1.04	0.96	0.96

Note: Comparison of "Wu-Xia (plug-in VAR)" (baseline, in denominator) against "Shadow-rate VAR." Values below 1 indicate improvement over baseline. Evaluation window from 2009:01 through 2020:09. Significance assessed by Diebold-Mariano-West test using Newey-West standard errors with $h+1$ lags. Due to the close behavior of some of the models compared, and rounding of the reported values, one of the comparisons shows a significant ratio of 1.00. This case arises from persistent differences in performance that are, however, too small to be relevant after rounding.

Figure 1: Interest rate data

(a) Full data sample

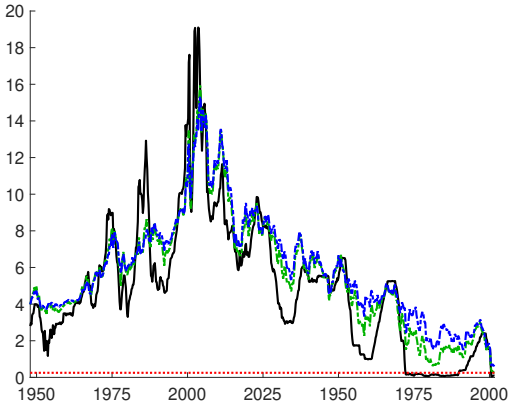

(b) Since the GFC

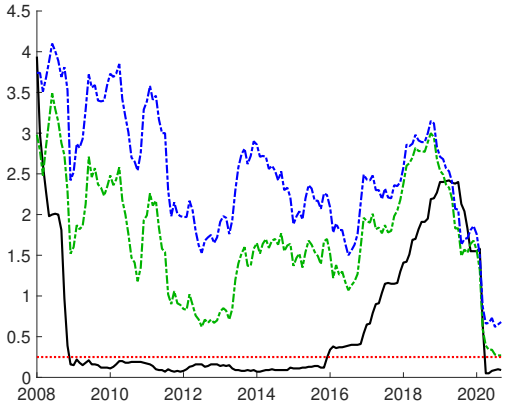

Note: All interest rates quoted as annualized percentage rates. Data obtained from FRED-MD; for further details see section 3.

Figure 2: Shadow-rate estimates

(a) Full-sample vs quasi-real time

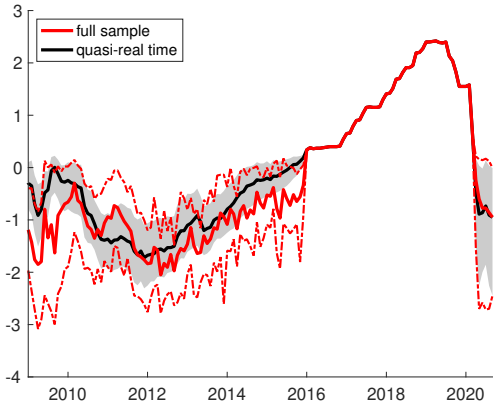

(b) Other shadow-rate estimates

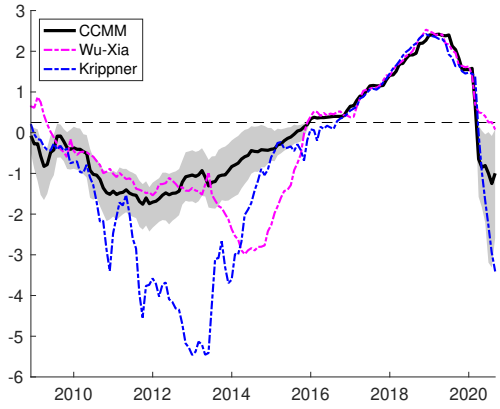

Note: Panel (a) compares smoothed and quasi-real time shadow-rate estimates from our baseline shadow-rate VAR. The quasi-real-time estimates are the end-of-sample estimates produced by recursive estimation of the model starting in January 2009. Each estimation conditions on available data since 1959:03, but the figure omits the period prior to 2008 during which the ELB did not bind. Posterior medians are shown as thick lines; grey shaded areas and thin lines depict 90 percent uncertainty bands. Panel (b) compares the smoothed shadow-rate estimates (also shown in Panel (a)) against updated estimates obtained from Krippner (2013, 2015) and Wu and Xia (2016).

Figure 3: Effect of imposing ELB on shadow-rate estimates

(a) Missing-data and shadow-rate draws

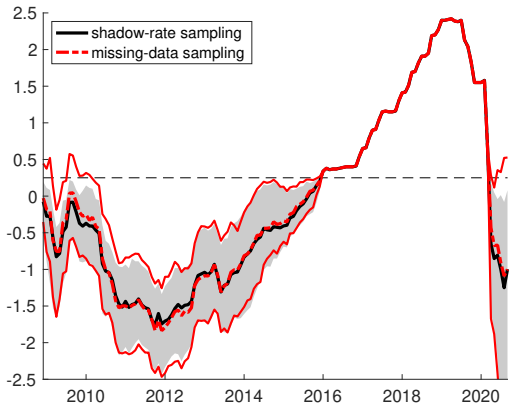

(b) Missing-data draws from different VARs

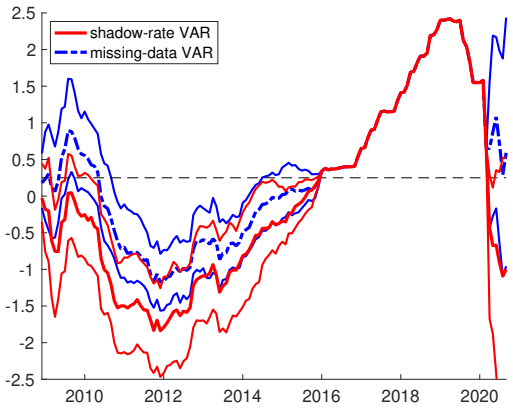

Note: Panel (a) compares shadow-rate (black) and missing-data (red) draws for s_t obtained from the posterior of our baseline shadow-rate VAR. Shadow-rate draws are obtained from the truncated posterior for s_t that satisfies the ELB. Missing-data draws are obtained from the underlying (and untruncated) posterior of the missing data problem that ignores the ELB. Panel (b) displays missing-data posteriors obtained from two sets of VAR estimates: In the baseline (red), parameter and SV draws reflect shadow-rate sampling. In the alternative version (blue), parameters and SV are drawn while treating the policy rate at the ELB as missing data and without requiring that missing data draws lie below the ELB. In this panel, medians are reported as thick lines and 90 percent uncertainty bands are reported with the grey shaded area or thin lines.

Figure 4: Predictive densities for the federal funds rate

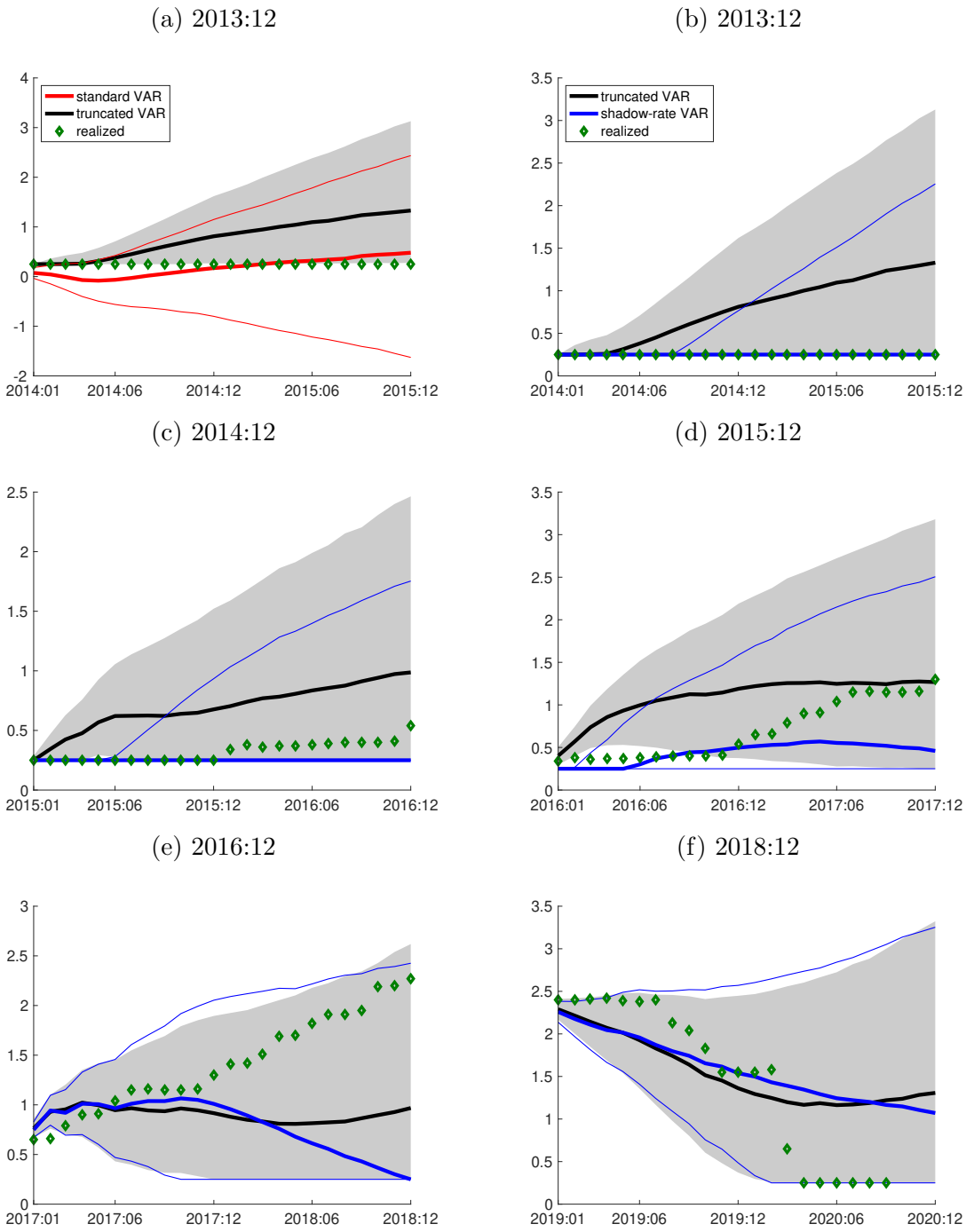

Note: Predictive density for the federal funds rate, simulated out of sample at different jump-off dates for different models. Panel (a) compares predictions from the standard VAR against those from the truncated VAR. The remaining panels compare predictions from the truncated VAR against those from the shadow-rate VAR. Realized values for the federal funds rate are shown as green diamonds and were set equal to the ELB value of 25 basis points from 2008:12 until 2015:12, and then again as of 2020:04.

Figure 5: Predictive densities for shadow and actual rate

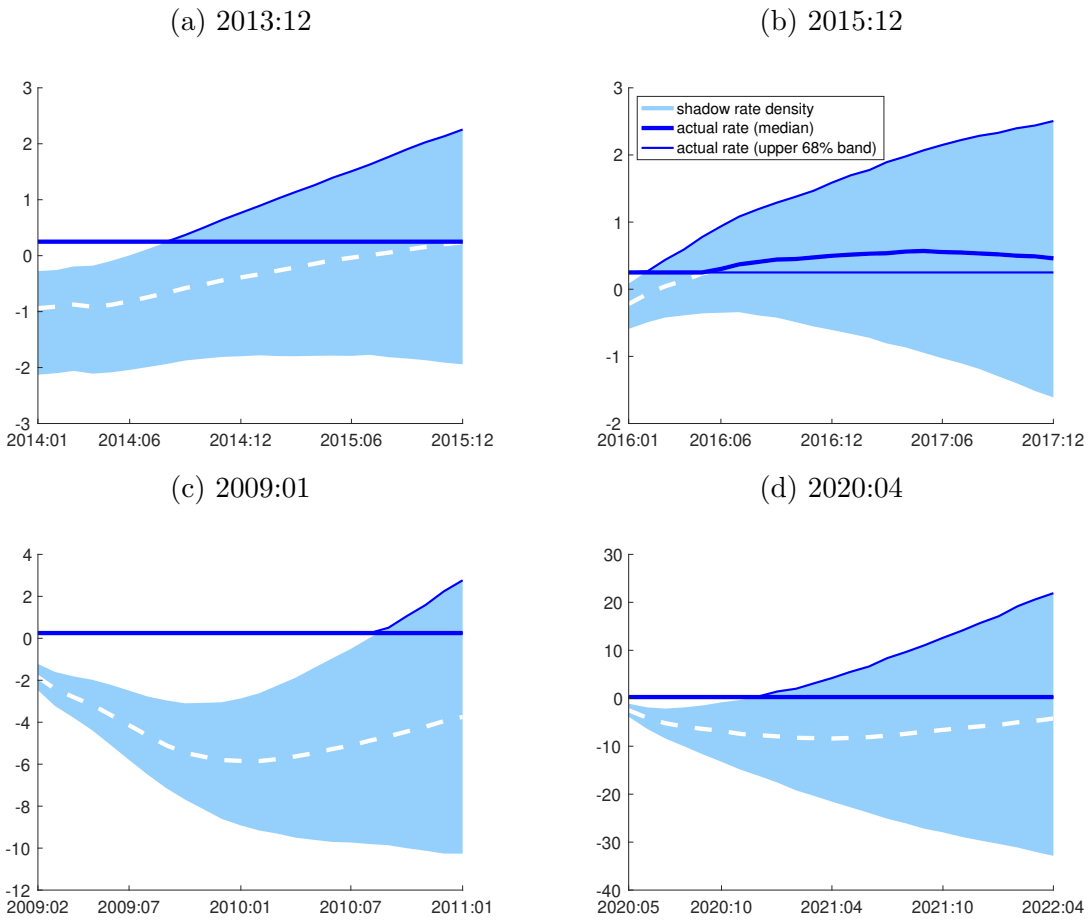

Note: Predictive density for the shadow rate (shaded area, light blue) and actual federal funds rate (solid lines, dark blue), simulated out of sample at different jump-off dates from our baseline shadow-rate VAR. The medians of the predictive densities are shown as thick lines (shadow rate: white dashes, actual federal funds rate: dark blue). The 68 percent bands are shown as shaded areas (shadow rate), and thin solid lines (actual federal funds rate), respectively. For the actual rate, the 68 percent bands collapse to the ELB of 25 basis points, when the corresponding bands of the shadow-rate density lie entirely below the ELB.

Figure 6: Predictive densities for the federal funds rate in 2020

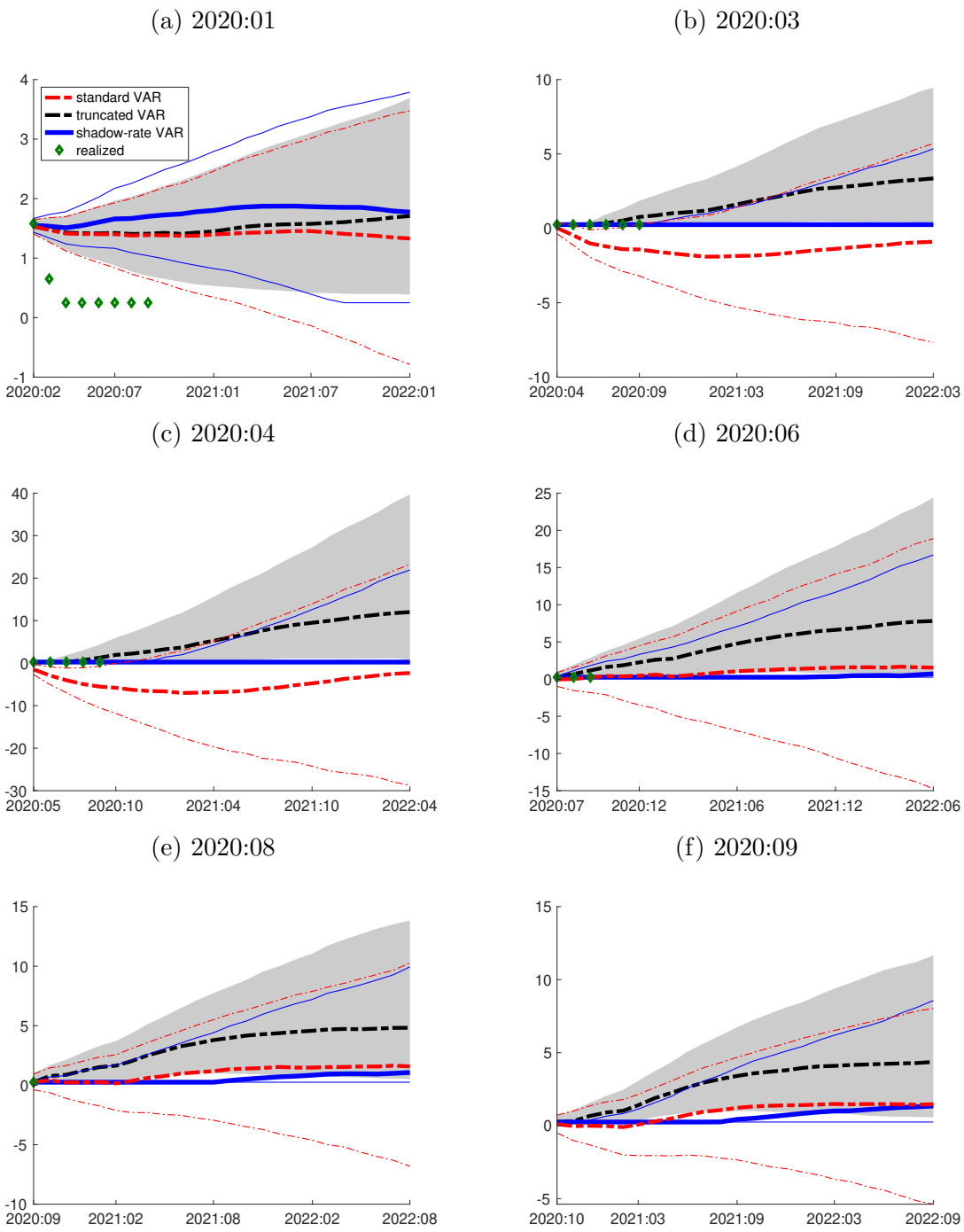

Note: Predictive density for the federal funds rate, simulated out of sample at different jump-off dates for different models. Realized values for the federal funds rate are shown as green diamonds (set equal to the ELB value of 25 basis points as of 2020:04).